[AMERICAN JOURNAL OF SCIENCE, VOL. 278, NOVEMBER, 1978, P. 1185-1234]

American Journal of Science

NOVEMBER 1978

EXPERIMENTAL STUDIES OF CHANGES PRODUCED BY DEPOSIT FEEDERS ON PORE WATER, SEDIMENT, AND OVERLYING WATER CHEMISTRY

ROBERT C. ALLER*

Department of Geology and Geophysics,
Yale University
New Haven, Connecticut 06520

ABSTRACT. Two separate sets of laboratory experiments were performed to study the changes produced by deposit-feeding organisms in marine sediment and overlying water chemistry. The organisms used: *Clymenella torquata*, a sedentary tube dweller, and *Yoldia limatula*, a mobile subsurface deposit feeder, are representative of two important and distinctive deposit-feeding groups. Both species produce radical changes in pore-water profiles of Fe and Mn and increase the sediment-water flux of these metals. *Clymenella* did not feed during the experiment. Alterations of pore-water profiles compared to controls in this case are best explained by changes, brought about by burrow construction and irrigation, in the geometry of molecular diffusion in sediment. A non-steady-state *radial*-diffusion model is used to characterize transport geometry. On the other hand, *Yoldia limatula* is highly mobile, and pore-water transport in its presence can be characterized by a non-steady-state, composite-layer model in which an effective or biogenic diffusion coefficient acts in the zone of feeding, and molecular diffusion controls transport in underlying sediment. Pore water and flux data show that the effective biogenic diffusion coefficient for pore-water transport by *Yoldia* is $\sim 1 \times 10^{-5}$ cm^2/sec. Modeling of interstitial metabolites and solid phase properties also shows that *Yoldia* increases the rate of microbial metabolic activity and associated reactions in sediment, but that alteration of effective diffusion rates is most important in controlling pore water profiles. Control experiments indicate that $HPO_4^=$ and HCO_3^- are consumed near the sediment-water interface by adsorption on Fe-oxides and oxidation of sulfides respectively. $CaCO_3$ is also dissolved in the same region, at a rate of $\sim$9 mg/g sediment-yr, producing a Ca^{++} maximum in pore water. These abiogenic reactions are largely masked in the presence of *Yoldia* by increased biogenic diffusion. Solid-phase Mn profiles typical of natural deposits are found to form on time scales of a month and to be influenced by *Yoldia* in accordance with the chemical behavior expected for Mn and the changes in transport caused by *Yoldia*. Production rates of dissolved Mn are 2 to 4 times higher in the presence of *Yoldia* than in its absence. The transport of particles and pore water during feeding, burrowing, and irrigation of sediment by both *Yoldia* and *Clymenella* influences different pore-water and solid-phase constituents to a variable degree consistent with their individual chemistry. In general, the effect of both organisms is to speed the rate of transfer between chemical reservoirs while at the same time masking the presence of specific reactions which would otherwise be expressed in standing concentrations of dissolved ions in interstitial or overlying water.

INTRODUCTION

The influence of a given deposit-feeding species on sediment properties depends on its taxonomic group, size, mobility, life habit, particle

* Present address: Department of the Geophysical Sciences, University of Chicago, 5734 South Ellis Avenue, Chicago, Illinois 60637

size selectivity, depth and rate of feeding, and the population densities in which it normally occurs. In this study, two species, representing two very different and important functional groups of marine deposit-feeding organisms, have been examined in the laboratory for their effects on selected aspects of chemical diagenesis near the sediment-water interface.

One of these species is *Yoldia limatula,* a siphonate, protobranch bivalve which occurs commonly in shallow sub-tidal muds off the northeast coast of North America (fig. 1A). The protobranchs are small (0.1-4 cm), highly mobile, and generally feed below the sediment-water interface but within the top 2 to 4 cm (Stanley, 1970; Levinton and Bambach, 1975). They are conspicuous and abundant enough that a protobranch species is sometimes used as a characteristic species in the classification of bottom communities, for example, the *Yoldia limatula-Nephtys incisa* community of Long Island Sound (Sanders, 1956). They are active, which together with natural population densities of several hundred per m^2 results in high rates of particle reworking in bottoms where these animals are present (Rhoads, 1963; Young, 1971; Aller and Cochran, 1976). Because of this biogenic activity and the resulting changes in mass properties and physical stability of the bottom, protobranchs are thought to play a significant role in determining the distribution of other organisms (Rhoads and Young, 1970).

The other species investigated in this study is *Clymenella torquata,* a maldanid polychaete which normally inhabits muddy sands along the east coast of North America (fig. 1B). Maldanids orient vertically in the sediment, ingest particles at depths from 10 to 30 cm, and pass them vertically to the sediment surface (Mangum, 1964; Rhoads, 1967). In this respect they are functionally representative of many deposit feeders that orient and feed in a similar way. *Clymenella* is capable of reburrowing if

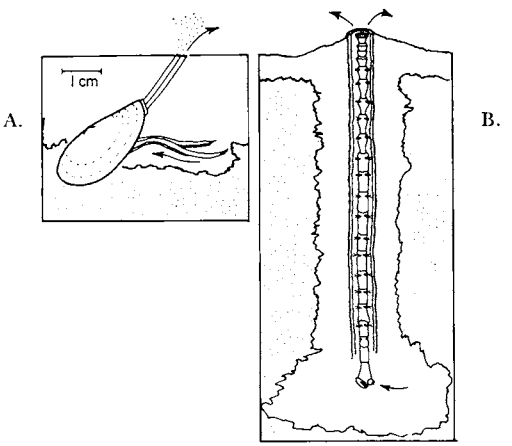

Fig. 1. A. Sketch of *Yoldia limatula* in feeding position, labial palps extended. Unstippled region represents visually oxidized sediment. Arrows indicate direction of particle transport. B. *Clymenella torquata* in tube. Unstipled sediment represents oxidized zone; arrows indicate transport direction of particles.

exumed but under normal conditions tends not to be highly mobile. Maldanids are tube-dwellers; *Clymenella* constructs a permeable, lined-tube of poorly sorted sand grains while other maldanids such as *Maldanopsis* may form less permeable, firmly packed tubes of mud. Maldanids are common members of near-shore and deep-sea bottom communities.

Many of the effects of deposit-feeding organisms on sediment chemistry result from the changes that these animals produce in the transport processes occurring in a deposit. These changes can be divided into those predominantly involving the transport of either particles or fluid. Feeding, burrowing, and construction activity influence particle transport while fluid transport is affected mostly by irrigation (for respiration) and burrowing. Changes in selected aspects of *average* sediment chemistry which accompany biogenic transport activity are investigated in this study. Changes resulting from the formation of tube microenvironments (Aller and Yingst, 1978) or indirect changes caused by synergistic interaction between macro- and microfauna are also considered but given less emphasis.

Fe and Mn were chosen for special study for several reasons: (1) These metals are believed to have a dominant role in determining the distribution and mobility of many other metals such as Cu, Zn, Co, and Ra (for example, Goldberg, 1954; Krauskopf, 1956; Jenne, 1968). (2) Both Fe and Mn are highly sensitive to oxidation-reduction conditions and the presence of sulfide and are thereby particularly sensitive to diagenetic processes involving the destruction of organic matter by O_2 or $SO_4^=$ reduction. Reactions of this type are especially rapid in the near interface zone inhabited by benthos and can be expected to be influenced by the activities of the animals dwelling there. (3) As a result of the conditions mentioned above, Fe and Mn are present in sufficient concentrations in sediment pore water to be readily measured without extensive preconcentration.

In addition to Fe and Mn: NH_4^+, $HPO_4^=$, $SO_4^=$, pS, and alkalinity were also measured in some cases. These constituents are useful indicators of decomposition and metabolic processes, are potential reactants with Fe and Mn, and are important nutrients. The similar sources (organic material) but different reactivity and chemistry of NH_4^+ and $HPO_4^=$ also allow the tracing in certain cases of reactions involving their differential precipitation or other mechanisms of their removal, such as adsorption.

METHODS

Experiments consisted basically of comparing pore water profiles, sediment, and overlying water chemistry in seawater aquaria containing animals, with aquaria in which macroorganisms were absent (controls).

Experiments with Yoldia limatula.—*Yoldia limatula* and sediment were collected at station NWC in Long Island Sound, 6 km south of the New Haven Harbor entrance on October 21, 1975 (see Rhoads, Aller, and Goldhaber, 1977). Samples of the upper ~10 cm of sediment were

taken by grab and placed in polyethylene containers. *Yoldia* were removed as they came near the surface of the samples and placed temporarily into a holding tank. The wet sediment, which is > 75 percent silt-clay, was then forcibly passed through a 1 mm sieve to remove other macrofauna and large shells debris. No additional water beyond that naturally in the sediment was added. This sieved sediment was homogenized and placed as a 10 cm deep layer in each of two plexiglas tanks having dimensions of 28.7 × 29.7 × 30.5 cm for width, length, and height. The tanks were then carefully filled with water, 30 *Yoldia* added to one tank, aerators inserted, and then the top partially sealed with a glass plate. This was all completed on the same day as collection. Temperature was subsequently maintained at 22°C. Collection site temperature at this time of year is ~17°C.

A sample of the starting sediment was taken and processed for pore water analysis as follows. Sediment was packed into a 10 cm long section of butyrate tubing (4.5 cm I.D.), then squeezed using the method of Kalil and Goldhaber (1973). Pore water was expressed first through glass fiber filters followed by 0.45 μm pore size Millepore filters directly into plastic syringes without air contact. Water was analyzed for $SO_4^=$, NH_4^+, $HPO_4^=$, alkalinity, Ca, Cl^-, Fe, and Mn. ($Si(OH)_4$ was also measured, but the results will not be described in this report.) $SO_4^=$ analyses were made on 10 ml samples. A 10 ml sample was taken for alkalinity, Fe, and Mn determination as follows. Immediately after filling of the sample syringe the pore water was transferred through a short section of tygon tubing into a 10 ml pipet. This pipet was drained directly into an acid-cleaned and thoroughly rinsed 2 oz polyethylene wide-mouthed bottle; total transfer time was approx 30 sec. Alkalinity titrations were then made directly in this vial, and the samples acidified to pH ~ 1.5 to 2. After sitting for at least a week following acidification, these samples were analyzed for Fe and Mn as described under analytical techniques below. No significant Fe or Mn blank or loss (recovery 100 ± 1 or 2 percent for Fe and Mn respectively) is incurred by this method, if titration and acidification are performed within about 1 week after transfer (Aller, 1977). Samples for $HPO_4^=$, NH_4^+, and Cl^- were taken in 3 cc syringes and analyzed as described below.

Overlying water in each tank was changed at approx 1 week intervals. Water samples were taken by inserting a piece of Tygon tubing below the water surface in each tank and drawing water directly into a syringe. An inline filter holder was attached, and water filtered directly through a 0.4 μm pore size Nuclepore filter into acid-cleaned polyethylene sample bottles. Water used for Fe and Mn determinations was acidified to 0.1 N HCl immediately. Filtered samples for $HPO_4^=$ and NH_4^+ analyses were placed in a refrigerator (4°C) and either analyzed or fixed, in the case of NH_4^+, within 24 hrs. Samples for Cl^- analysis were titrated immediately.

After 6 weeks the tanks were drained and inserted directly into a glove bag. The bag was pumped down with a vacuum pump and flushed

with N_2 several times. Sediment was carefully removed at 1 or 2 cm intervals by use of plastic spoons and placed in precut 10 cm sections of butyrate tubing (4.5 cm I.D.). *Yoldia* were picked out during sampling, although some may have escaped notice. The pH and pS were measured by insertion of electrodes directly into the upper portion of the sample, and the tube then sealed with end caps. A portion of sediment from each depth was taken for H_2O content and ATP determination. When all intervals had been sampled and tubes sealed, the glove bag was opened, and the samples were removed and placed into a refrigerator (4°C) for storage prior to squeezing. Pore water was removed by the method of Kalil and Goldhaber (1973), and samples treated as described previously. Squeezing was completed within 12 hrs of sampling; sediment was allowed to come to room temperature (22°C) before squeezing.

Experiments with Clymenella torquata.—*Clymenella* and sediment from their natural habitat were collected at Calves Pasture Point, Barnstable Harbor on Cape Cod, Mass., and transported to Yale University, New Haven, Conn. Collections during 1972 and 1973 showed that these organisms were easily maintained alive in the laboratory for periods longer than 6 months. All animals used in the experiments described below were collected on June 29, 1974 and introduced to experimental tanks within 1 day of capture.

The muddy sand from the collecting site was dried, sieved through a 2 mm mesh sieve, then mixed with mud from New Haven Harbor (Long Wharf), Conn. in a ratio of 15 parts sand/1 part mud in order to increase the organic matter content of the sediment and raise the concentration of the elements measured to detectable levels in the sediment pore water. Sediment layers 15 cm deep were deposited in small increments (to prevent graded bedding) in each of four plexiglas aquarium tanks and covered with seawater for 12 days prior to the start of the experimental run. These aquaria had dimensions of 33.3 × 29.1 × 33.3 cm for length, width, and height and were each connected by latex rubber tubing to separate 50 *l* polyethylene carboys, the outside of which were painted black (fig. 2). The carboys acted as seawater reservoirs for

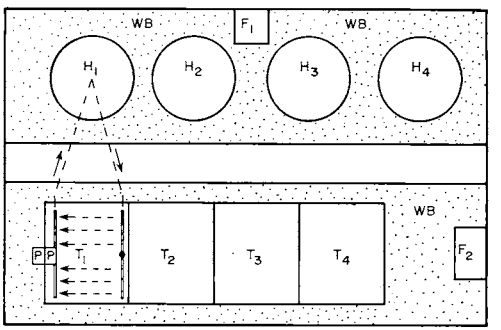

Fig. 2. Plan view of tank set up used in *Clymenella* experiment. H_i = holding tanks, T_i = aquaria, F_i = refrigerating units, WB = water bath (stippled), PP = pump. Path of water circulation is shown only for tank 1.

each tank, and water was continually circulated between the reservoir and its associated tank using a centrifugal pump (no metal parts in water contact) and a gravitational return. Sheet-like flow over the sediment surface was maintained by using perforated, pyrex glass tubes at each end of the tank for uptake and return of water. Salinity of the seawater was in the normal range found in the Barnstable Harbor collection area (see Aller and Yingst, 1978). Both the carboys and aquaria were surrounded by a water bath which kept the temperature at 19 ± 1°C. The entire system was placed under a polyethylene tent to prevent contamination by dust.

After an initial equilibration period of 12 days, the water over the tanks was changed. Water was then circulated and monitored for pH, Cl^-, $HPO_4^=$, NH_4^+, Fe, and Mn for an additional 2 week period in each tank. At the end of this 2 week period, tanks 1 and 2 were designated controls, and tanks 3 and 4 designated to receive *Clymenella*; tank 2 was drained at this time, and the sediment cored using a PVC coring tube. The core was immediately placed in a glove bag, and the bag flushed repeatedly with N_2. The core was then extruded in 1 cm intervals into specially constructed plastic squeezers made from syringes. These squeezers were sealed and then mounted into vises, and pore water mechanically squeezed out directly through 0.4 μm pore size Nuclepore membrane filters, which had been previously flushed with N_2, into 3 cc syringes. Syringes were weighed, and pore water expressed into 10 ml volumetric flasks where it was immediately acidified with 0.1 ml of HCl and diluted to 10 ml. Syringes were reweighed, and the amount of pore water obtained by difference. Great care was taken to prevent air contact with pore water during handling and squeezing prior to acidification. This minimizes loss of Fe due to oxidation and precipitation (Troup, Bricker, and Bray, 1974).

On the same day that tank 2 was sampled, 30 *Clymenella torquata* (a natural density of 300/m^2 comparable to the collection site) were placed in both tanks 3 and 4; tank 1 continued as a control tank. Overlying water was sampled during the following 2 week period at the end of which tanks 1 and 3 were cored and sampled as described above for tank 2. Cores taken in tank 3 were positioned to avoid burrows. Sediment from tank 4 was not sampled.

Analytical techniques.—pH was determined by direct insertion of a rugged, combination electrode into either a sediment or overlying water sample after standardization of the electrode in 7.414 buffer followed by rinsing. Measurements of pS were made by insertion of a standardized Ag_2S electrode (Berner, 1963) into sediment using the Ag/AgCl portion of the pH electrode as reference. In the case of sediment, these measurements were made directly in the glove bag by passing the lines through a sealed port in the side of the bag. The portion of sediment in which the electrodes were inserted in the squeezing tubes was eventually removed just before squeezing during the emplacement of glass fiber filters and squeezing caps.

All Fe analyses were made with the colorimetric reagent Ferrozine using a modification of the procedure of Stookey (1970); samples were not boiled but were reacted at room temperature for 1 hr prior to color development. Mn analyses were made using three different methods: formaldoxime colorimetric method (Goto, Komatsu, and Furukawa, 1962), a modified leuco malachite green colorimetric method (Strickland and Parsons, 1969; Aller, 1977) and atomic absorption spectrometry. Intercomparison of these methods on tap water and standard rock samples gave results within 5 percent of one another. Formaldoxime was used for analysis of Mn in all overlying water samples, leuco malachite green for pore water Mn samples in the *Clymenella* experiment, and atomic absorption was used for pore water Mn analysis in the *Yoldia limatula* experiment. All $HPO_4^=$ determinations were made using the molybdate method (Strickland and Parsons, 1969; Presley, 1971). NH_4^+ was analyzed by use of the phenolhypochlorite method after initial fixing with phenol (Solórzano, 1969; Degobbis, 1973). Cl^- was determined by $AgNO_3$ titration using chromate or starch-fluorescein indicators. Alkalinity was determined by titration with 0.1 N HCl (Gieskes and Rodgers, 1974). $SO_4^=$ was analyzed gravimetrically following precipitation of acidified samples with $BaCl_2$.

Estimates of percentage of organic matter were made by ignition of sediment at 475°C (~12 hrs) after drying to constant weight at 100°C. Percent H_2O was determined by drying sediment to constant weight at 80°C.

Mn determinations were made on aliquots of ashed sediment by heating for 24 hrs in 12 N HCl (30 ml), taking to near dryness, picking up in 0.2 N HCl, and filtering through Whatman 42 paper. The resulting leachate was diluted to known volume and analyzed for Mn by use of AA.

ATP analysis was done on wet sediment by J. Yingst. Sediment samples, with and without the addition of standard, were extracted in boiling bicarbonate buffer (Christian, Bancroft, and Wiebe, 1975), and ATP leached from the samples was determined by reaction with luciferin-luciferase (luminescence assay). Extraction efficiency was determined using the standard addition; average yield and total precision for this analysis are 108 ± 24 percent (Yingst, 1978).

RESULTS

Yoldia *experiment, sediment description.*—The sediment surface in the tank containing *Yoldia* was flocculent and watery (table 1) compared to the control. Protobranchs are known to increase the water content of fine-grained sediment during reworking (Rhoads and Young, 1970; Young, 1971).

Except for some very minor disturbance by meiofauna, the control tank maintained surface features that were formed when sediment was laid down in each tank. In comparison, the *Yoldia* tank surface sediment was composed of gently sloping fecal mounds and loosely aggregated

pellets with no hint of the original flat surface. In section, the control tank sediment was capped by an orange-yellow oxidized layer 0.3 to 0.4 cm in depth underlain by black colored sediment. The color stratigraphy of the *Yoldia* tank was similar, except that the surface yellow zone was 2 to 3 cm thick.

Yoldia *experiment, pore water.*—Analytical results of pore water and solid phase analyses in the *Yoldia* and control tanks are listed in table 1 and graphed as depth dependent concentration profiles in figures 3 and 4; initial values, when available, are usually graphed for comparative purposes. Differences between *Yoldia* and control tanks are subtle in some instances but dramatic in others. Sulfate profiles show definite depletion of seawater sulfate with depth in both tanks; normalization to Cl^- does not significantly change this observation. The *Yoldia* tank has slightly higher sulfate concentrations in the upper 5 cm and slightly lower values from 5 to 9 cm depth interval compared to the control, but these differences are not analytically significant. Decreasing $SO_4^=$ is mirrored by decreasing pS values with depth in both tanks, with slightly lower pS below 5 cm in the *Yoldia* tank than control (table 1).

Associated with decreases in sulfate are increases in interstitial concentration of alkalinity, ammonia, and phosphate (fig. 3). These trends

TABLE 1

Yoldia tank experiment: pore water and sediment

	Pore Water										Sediment		
Depth (cm)	$\%H_2O$	pH	pS	Cl^- (M)	Alk (meq/l)	$SO_4^=$ (mM)	NH_4^+ (μM)	$HPO_4^=$ (μM)	Ca (mM)	Mn (μM)	Fe (μM)	Ignition loss(%)	ATP (μg/g)	Mn (μg/g-ash)
Control														
0-1	61.6	7.45	-	0.539	4.45	28.3	62	5	10.75	33.5	1.1	5.99	0.503	694
1-2	57.0	7.14	-	0.534	4.80	27.3	135	20	11.56	72.8	55.9	6.08	1.67	589
2-3	56.2	7.03	-	0.526	5.47	26.5	208	34	11.92	91.0	91.5	6.30	1.32	600
3-4	54.2	7.02	-	0.515	6.11	24.3	256	49	11.83	105	61.8	6.52	1.43	620
4-5	54.4	7.15	14.2	0.509	7.49	23.6	372	86	10.78	109	7.31	6.35	0.685	631
5-7	54.2	7.27	12.4	0.501	8.28	23.5	420	97	10.36	101	4.28	6.47	0.812	615
7-9	53.8	7.40	13.2	0.494	8.93	22.3	497	112	9.82	81	2.9	6.37	0.23	603
Yoldia														
0-1	69.3	7.16	-	0.546	3.07	28.5	63	6.9	10.12	17.5	0.91	6.23	0.552	647
1-2	60.3	7.19	-	0.543	3.60	28.1	133	20	10.09	48.9	4.06	5.92	1.84	538
2-3	56.6	7.15	-	0.534	4.15	27.0	183	32	10.39	61.3	4.62	5.89	1.29	608
3-4	53.4	7.27	-	0.519	4.21	25.2	290	65	9.40	67.5	2.3	5.65	1.01	605
4-5	53.7	7.36	12.5	0.515	5.94	24.1	374	90	9.31	74.4	2.1	6.44	1.51	607
5-7	53.5	7.35	11.5	0.505	6.74	23.5	453	114	9.25	69.2	2.1	6.33	1.50	637
7-9	53.5	7.37	11.9	0.493	7.48	22.2	507	113	8.75	66.4	1.8	6.17	1.34	596
Initial Values														
-	-	7.49	*	0.457	3.72	22.8	217	65.2	8.89	73.5	1.7	(5.92)	-	617

* not measured

are predictable results of nutrient regeneration resulting from the decomposition of organic matter during sulfate reduction (for example, Richards, 1965; Goldhaber and Kaplan, 1974). Alkalinity concentrations are lower at all depths in the tank containing *Yoldia* than in the control. The profile in the *Yoldia* tank shows a break in concentration gradient at ~3 to 4 cm, while the control tank profile is slightly bowed from a smoothly increasing profile to lower values in the region from 2 to 4 cm, yielding a profile shape similar to that present in the *Yoldia* tank. The ammonia profiles are similar in both tanks, but some distinct differences do occur. Above 3 cm, NH_4^+ concentrations are the same or lower in the *Yoldia* side than the control, below 3 cm the *Yoldia* tank invariably has higher concentrations. This results in a slight break in the depth trend of concentration at ~3 cm in the *Yoldia* tank. Phosphate concentrations show the same trends and differences between tanks as does ammonia, except a definite bowing or concavity in the profiles of both tanks can be noticed above 4 cm.

Dissolved Mn profiles are similar in shape in both tanks in the sense that in both the concentration of Mn increases to a maximum at 4 to 5 cm and then decreases below that interval. The tanks differ in

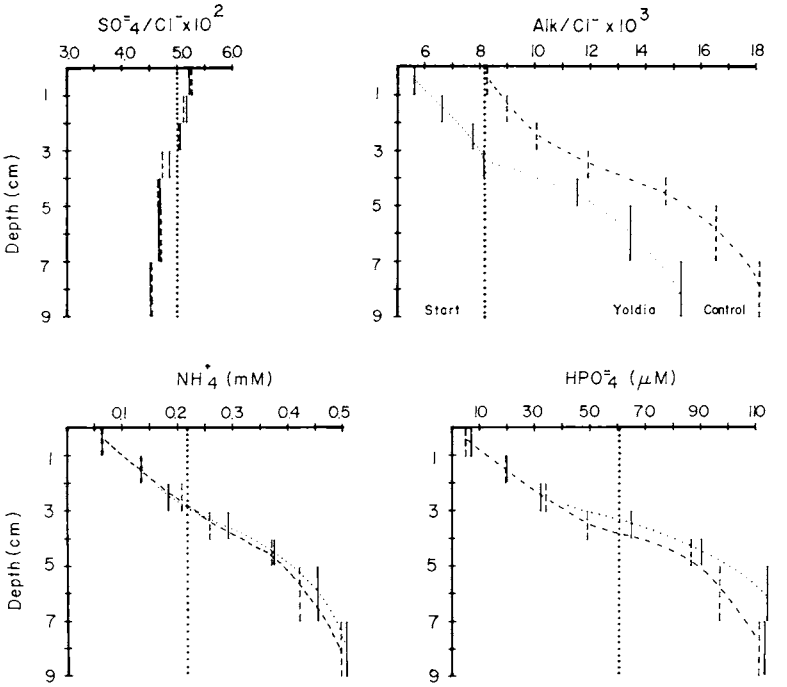

Fig. 3. Pore water sulfate, alkalinity, NH_4^+, and $HPO_4^=$ profiles from *Yoldia* experimental tanks. Control tank = dashed lines; *Yoldia* tank = solid lines, dotted profile; starting value = large dots.

that Mn concentrations are lower at every depth in the tank containing *Yoldia* than in the control (fig. 4; table 1).

In the same way, dissolved Fe profiles are similar in basic depth trends: increasing to a maximum followed by decreasing concentration at depth, but concentrations are higher in the control (fig. 4; table 1). This is especially true in the region of the maximum value from 2 to 3 cm, where dissolved Fe is dramatically higher in the control.

Like Fe and Mn, Ca in the control increases to a maximum concentration at a depth of 3 to 4 cm then decreases below that interval (fig. 4). Ca values have been normalized to Cl^- to show that Ca increases beyond seawater Ca/Cl ratios (~0.0187) at all depths in the control tank and in the upper 3 cm in the *Yoldia* tank.

The depth dependence of pH differs considerably in the two tanks (fig. 4; table 1). In the control, pH reaches a very low minimum value of 7.02 at 3 to 4 cm with sharply increasing values above and below. pH is relatively low and constant in the upper 3 cm of the *Yoldia* tank and then increases abruptly at 3 to 4 cm followed by a slower increase with depth.

Yoldia *experiment, solid phase properties.*—The distribution of organic matter differs in the two tanks and, in both, underwent change

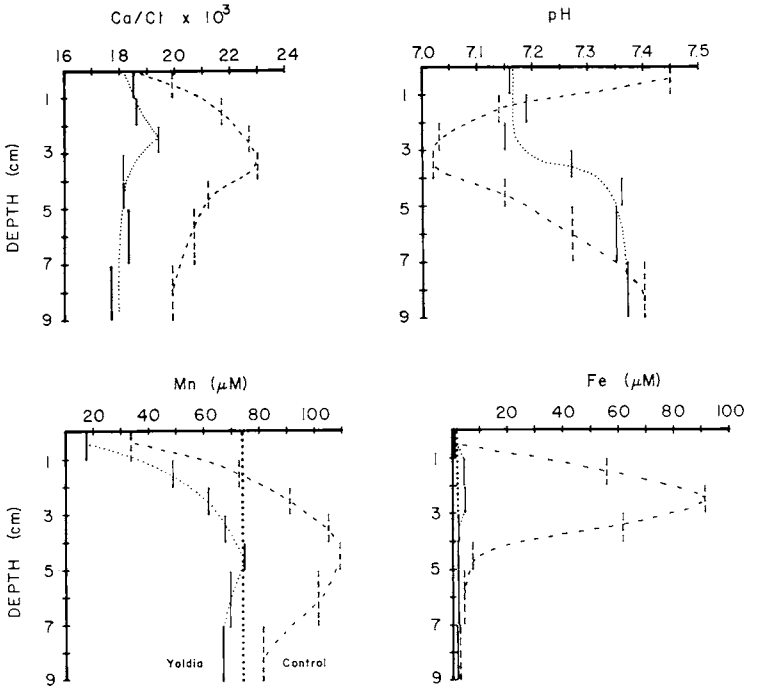

Fig. 4. Pore water Ca, pH, Mn, and Fe profiles from *Yoldia* experimental tanks. Control tank = dashed lines; *Yoldia* tank = solid lines, dotted profile; starting value = large dots.

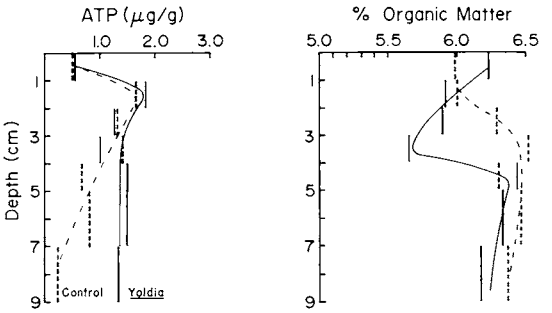

Fig. 5. ATP and % organic matter profiles from *Yoldia* experimental tanks. Control tank = dashed lines; *Yoldia* tank = solid lines.

from the initial value (fig. 5; table 1). In the *Yoldia* tank the organic matter profile was changed from initially constant with depth to one that decreases steadily from a surface maximum to a low at 3 to 4 cm, then jumps to a higher value which is maintained to depth. This higher value at depth is greater than the initial starting value. The control tank increases, below the interface, to a relatively high value similar to that found below 4 cm in the *Yoldia* tank.

ATP distribution (no correction for yield, see Methods) is similar in the upper few centimeters in the two tanks but shows distinct differences below 3 cm (fig. 5; table 1). In the *Yoldia* tank ATP reaches a local minimum at 3 to 4 cm and then increases to a relatively constant level independent of depth. The control profile reaches a slight maximum in the second cm and then decreases steadily to depth. No ATP values for the homogenized starting sediment were measured; typical ATP profiles at the sediment collection site are given in Yingst (1978).

Solid phase Mn (fig. 6; table 1) underwent a radical redistribution in the sediment during the 45 day experiment. Again, similarities and differences can be found between the tanks. Both have maximum Mn concentration in the top 0 to 1 cm, minimum levels at 1 to 2 cm, and then mild increases to a second maximum at depth followed by a de-

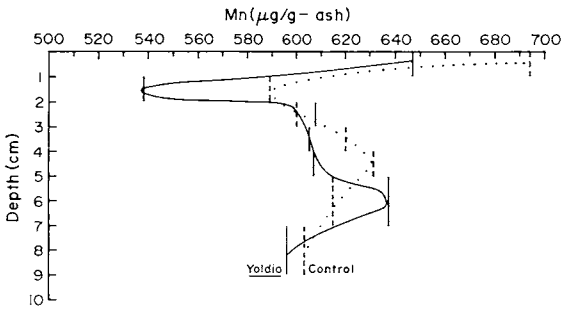

Fig. 6. Solid phase Mn profiles in *Yoldia* experimental tanks. Control tank = dashed lines; *Yoldia* tank = solid lines.

crease in concentration at the lowest sampling interval. Mn concentration profiles differ in that at most sampling intervals Mn is lower in the *Yoldia* than the control tank and that the interval in which the second maximum occurs is deeper in the *Yoldia* tank than control.

Yoldia *experiment, overlying water.*—A number of differences were found in overlying water properties and chemistry of the two tanks. The water in the *Yoldia* tank was continuously turbid throughout the experiment, and the sediment surface could not be seen from above. In the control, the overlying water was clear at all times.

Time dependent change in the concentration of total alkalinity, ammonia, phosphate, and Mn is plotted in figure 7, and additional data given in table 2. Plots are discontinuous at intervals, because water was changed at that time. In general, NH_4^+, $HPO_4^=$, and Mn concentrations increase after each water change. The rate of increase after each successive change decreases throughout the experiment in both tanks so that, in the case of Mn, little change occurs in overlying water concentrations toward the end of the experiment. The amount of increase of NH_4^+

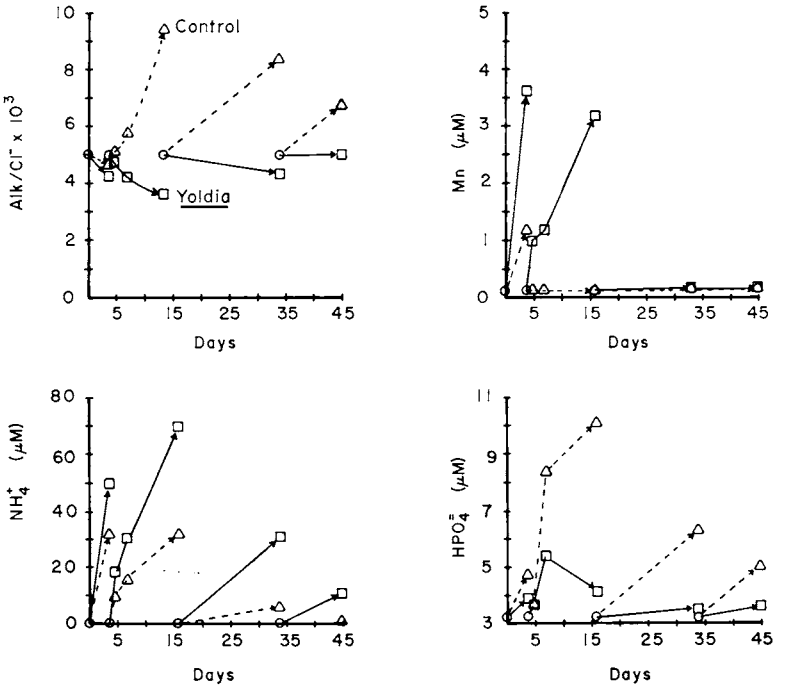

Fig. 7. Alkalinity/Cl^-, Mn, NH_4^+, and $HPO_4^=$ concentrations in overlying water of *Yoldia* experimental tanks with time. Control tank = open triangles, dashed lines; *Yoldia* tank = open squares, solid lines; source water used in each water change = open circles.

and Mn is greater in the tank with *Yoldia* than in the control, but $HPO_4^=$ increase is often greater in the control.

Changes in alkalinity levels of overlying water differed in general trends from NH_4^+, $HPO_4^=$, and Mn. At all times alkalinity decreased after each water change in the *Yoldia* tank, the magnitude of the decrease decreased through time. In the control tank, alkalinity decreased at first, then increased during all successive time intervals but at a decreasing rate. No associated change in Ca/Cl concentrations were found (table 2).

Clymenella *experiment, pore water.*—Pore water concentration profiles of both Fe and Mn underwent radical change in the presence of *Clymenella.* Prior to addition of animals, both metals had pore water concentrations that increased steadily with depth (fig. 8; table 3); this increase can be roughly approximated by a simple straight line. Comparisons of tank 2 with tank 1 data show that control tank profiles of dissolved Fe and Mn remained relatively stable over the 14 day period between samplings, but there is a tendency for somewhat lower values in tank 1. After addition of *Clymenella* in tanks 3 and 4, pore water concentrations became low at depth and high near the interface compared to the control tanks (fig. 8). Fe reaches a maximum in the second cm, while Mn continues to increase or stay the same in the top one cm. The deepest sampling interval, 9 to 10 cm, indicates that pore water values begin to increase again below that depth.

The measured dissolved Fe concentrations are high but not out of the range found in naturally accreting sediments (Bricker and Troup,

TABLE 2

Yoldia tank experiment: overlying water

Sample time (cumulative days)	Sample time (after water changes) days	Cl^- (M)			Alk (meq/l)			Ca (mM)		
		source water	Yoldia	Control	source water	Yoldia	Control	source water	Yoldia	Control
0	0	0.521			2.60			9.18		
3.6	3.6 (change)		0.520	0.523		2.20	2.45		8.98	8.96
4.6	1.0		0.521	0.524		2.48	2.65		9.08	9.06
6.9	3.3		0.524	0.528		2.24	3.05		9.13	9.18
15.9	12.3 (change)		0.536	0.529		1.96	5.02		9.41	9.58
33.9	18 (change)		0.559	0.546		2.43	4.58		9.86	10.2
44.9	11 (end)		0.548	0.540		2.74	3.66		9.91	9.91
		NH_4^+ (μM)			$HPO_4^=$ (μM)			Mn (μM)		
		source water	Yoldia	Control	source water	Yoldia	Control	source water	Yoldia	Control
0	0	0.0			3.23			<0.14		
3.6	3.6 (change)		50	32		3.92	4.79		3.63	1.18
4.6	1.0		18.8	9.98		3.72	3.74		1.0	<0.14
6.9	3.3		30.3	15.9		5.46	8.40		1.2	<0.14
15.9	12.3 (change)		70	32		4.17	10.1		3.2	<0.14
33.9	18 (change)		30.8	5.9		3.54	6.33		0.16	<0.14
44.9	11 (end)		11	0.7		3.6	5.0		0.15	<0.14

1975; Troup, 1974; Aller, 1977). Mn concentrations are well within the range found in natural sediments. The Fe/Mn ratio of ~100 is higher than the 10 to 20 found normally in sediment pore waters from Barnstable Harbor (Aller and Yingst, 1978), probably as a result of the addition of sediment from New Haven Harbor.

pH showed a decrease with depth in all tanks, and the average pH in both the control and *Clymenella* tanks also increased with time. In the presence of *Clymenella,* however, pH increased beyond the control values in the top 5 cm of sediment (fig. 9).

Clymenella *experiment, overlying water.*—Cl^- concentrations in the overlying water remained relatively constant throughout the experimental period; a minor increase in chlorosity of ~0.015 M (3 percent of starting value) took place over the 29 day period of measurement due to evaporation. There is no significant difference between tanks (table 4).

The pH of overlying water decreased from ~8.2 to ~7.4 in all tanks during the experimental run. The pattern of change is similar in all cases (fig. 10; table 4).

$HPO_4^=$ decreased initially in all tanks and remained at constant low values in control tanks 1 and 2. After addition of *Clymenella* in tanks 3 and 4, $HPO_4^=$ increased and then dropped slightly in the last sampling (fig. 10; table 4).

NH_4^+ was low and essentially constant or decreasing in each tank. Following the addition of *Clymenella* in tanks 3 and 4 a radical increase in NH_4^+ concentration in tank water took place (fig. 10; table 4), and this increase continued, but at a decreased rate, until the end of the experiment.

Dissolved Fe and Mn ($\leq$ 0.4 μm) were initially near or below the detection limits for the analytical methods in all tanks. They remained

TABLE 3

Clymenella tank experiment: pore water results

	pH				Fe (μM)			Mn (μM)		
Depth (cm)	Tank 1 (control t = 29)	Tank 2 (control t = 15)	Tank 3 (Clymenella t = 29)		Tank 1 (control t = 29)	Tank 2 (control t = 15)	Tank 3 (Clymenella t = 29)	Tank 1 (control t = 29)	Tank 2 (control t = 15)	Tank 3 (Clymenella t = 29)
			duplicate cores							
0-1	7.00	6.96	7.22	7.20	122	310	1190	4.0	4.6	22
1-2	6.93	6.89	7.22	7.24	657	757	2010	4.2	4.6	20
2-3	6.93	6.85	7.15	7.26	962	1340	160	5.3	9.5	2.7
3-4	6.93	6.83	7.00	7.15	1650	1060	110	11	13	2.4
4-5	6.92	6.82	6.96	7.04	1750	1574	150	14	16	2.7
5-6	6.91	6.80	6.94	6.95	1650	2220	39	14	16	<1.8
6-7	6.91	6.80	6.93	6.92	1950	2150	20	16	20	<1.8
7-8	6.89	6.78	6.91	6.89	2170	2600	9	18	24	1.8
8-9	6.89	6.76	6.91	6.90	1770	2360	160	21	29	1.8
9-10	6.88	6.72	6.90	6.90	-	3010	636	-	22	6.0
10-11	6.88	6.72	6.87	6.89	-	3800	-	-	25	-
11-12	6.83	6.63	-	6.85	-	-	-	-	-	-

low in the control tanks, but after addition of *Clymenella* to tanks 3 and 4 both Fe and Mn in overlying water increased (fig. 11; table 4). Like $HPO_4^=$, dissolved Fe decreased in the last sampling period after an initial large jump in concentration. Mn, like NH_4^+, continued to increase.

DISCUSSION

Pore water and sediment chemistry profiles in the experimental tanks result, like their natural counterparts, from competition between transport and reaction processes. These processes will be examined first for the mobile deposit feeder (*Yoldia*) experiment, and then results and interpretations compared with the sedentary tube-dweller (*Clymenella*) experiment.

Decomposition reactions in tank sediment.—Many of the observed changes in pore water chemistry and sediment color distribution in the *Yoldia* experiment are consistent with the decomposition of organic matter in tank sediment by sulfate reducers (see Richards, 1965; Goldhaber and Kaplan, 1974). The reactions can be described in a general way by the equation (Richards, 1965):

$$6(CH_2O)_x\,(NH_3)_y\,(H_3PO_4)_z + 3x(SO_4^=) \rightarrow 6x(HCO_3^-) + 6y(NH_3) + 6z(H_3PO_4) + 3x(H_2S) \quad (1)$$

The stoichiometry of C/N/P (x/y/z) in the metabolized fraction depends on the stage of decomposition and may vary as a function of depth and time in sediments (Sholkovitz, 1973). In the free state and at normal pH values of sediments, reaction products are present predominantly as NH_4^+, $HPO_4^=$, HS^-, and HCO_3^- (Berner, Scott, and Thomlinson,

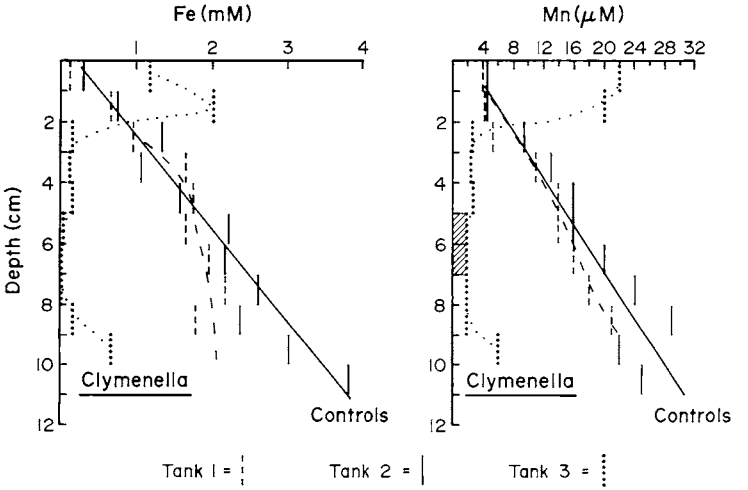

Fig. 8. Fe and Mn pore water profiles from tanks 1 (dashed lines), 2 (solid lines), and 3 (dotted lines) of *Clymenella* experiment. *Clymenella* present in tank 3.

1970; Kester and Pytkowicz, 1967; Goldhaber and Kaplan, 1975). Anaerobic remineralization reactions other than sulfate reduction must also take place in tank sediment, but these are probably less important under the experimental conditions and will be generally ignored in this discussion.

Depth dependence of decomposition reaction rates.—The rate and depth dependence of organic matter decomposition and therefore the production of interstitial metabolites in a deposit is related to the quantity of metabolizable organic matter present in a given depth interval (Zobell and Anderson, 1936; Waksman and Hotchkiss, 1938). In the case of decomposition of organic matter by $SO_4^=$ reducers, rates are known in many instances to decrease sharply with depth (for example, Zobell and Rittenberg, 1948; Oppenheimer, 1960; Sorokin, 1962; Goldhaber and others, 1977). This decrease is thought to depend predominately on depletion of reactive organic substrate.

At station NWC, where sediment was collected for the *Yoldia* experiment, the rate of sulfate reduction decreases exponentially with depth. The rate (22°C) can be approximately described in the top 10 cm by the expression: $R = 129 \exp(-0.33x)$ mM/yr (Aller and Yingst, in preparation). In the experimental tanks, sediment was thoroughly homogenized before beginning the experiment so that both quality and quantity of organic matter were initially constant with depth. This means that, to a first approximation, the initial rates of sulfate reduction or production of NH_4^+, $HPO_4^=$, HS^-, and HCO_3^- ($\sim$ alkalinity) can be assumed constant with depth. Such an assumption is important in the interpretations of the profiles given later.

Reactions associated with the production of dissolved Fe, Mn, and Ca will be discussed as required.

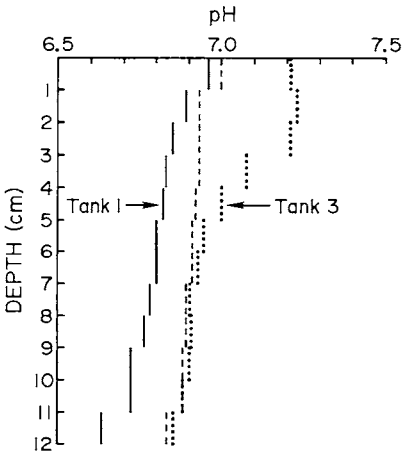

Fig. 9. pH profiles from tanks 1 (dashed lines), 2 (solid lines), and 3 (dotted lines) of *Clymenella* experiment.

TABLE 4

Clymenella tank experiment: overlying water

Time (days)	Measurement	Tank 1 (Control)	Tank 2 (Control)	Tank 3 (Clymenella)	Tank 4 (Clymenella)
0	pH	8.16	8.16	8.16	8.16
	Cl^- (M)	0.488	0.490	0.486	0.491
	$HPO_4^=$ (μM)	1.39	1.39	1.39	1.39
	NH_4^+ (μM)	1.22	1.22	1.22	1.22
	Fe (μM)	≤ 0.05	≤ 0.05	≤ 0.05	≤ 0.05
	Mn (μM)	≤ 0.14	≤ 0.14	≤ 0.14	≤ 0.14
9	pH	7.60	7.62	7.68	7.62
	Cl^- (M)	0.490	0.487	0.489	0.491
	$HPO_4^=$ (μM)	0.09	0.16	0.17	0.17
	NH_4^+ (μM)	0.92	-	-	1.29
	Fe (μM)	≤ 0.05	≤ 0.05	≤ 0.05	≤ 0.05
	Mn (μM)	≤ 0.14	≤ 0.14	≤ 0.14	≤ 0.14
15	pH	7.80	7.80	7.92	7.78
	Cl^- (M)	0.496	0.497	0.497	0.497
	$HPO_4^=$ (μM)	0.13	0.17	0.22	0.07
	NH_4^+ (μM)	1.00	0.57	0.84	1.35
	Fe (μM)	0.16	≤ 0.05	0.13	0.14
	Mn (μM)	≤ 0.14	≤ 0.14	≤ 0.14	≤ 0.14
16	Add Clymenella to tanks 3 and 4				
22	pH	7.53	-	7.38	7.38
	Cl^- (M)	-	-	-	-
	$HPO_4^=$ (μM)	0.19	-	0.54	0.47
	NH_4^+ (μM)	0.76	-	22.4	15.6
	Fe (μM)	0.11	-	6.21	0.20
	Mn (μM)	≤ 0.14	-	0.22	0.20
29	pH	7.40	-	7.39	7.38
	Cl^- (M)	0.502	-	0.507	0.503
	$HPO_4^=$ (μM)	0.10	-	0.51	0.43
	NH_4^+ (μM)	0.82	-	26.1	18.9
	Fe (μM)	0.11	-	1.95	5.17
	Mn (μM)	≤ 0.14	-	0.51	0.40

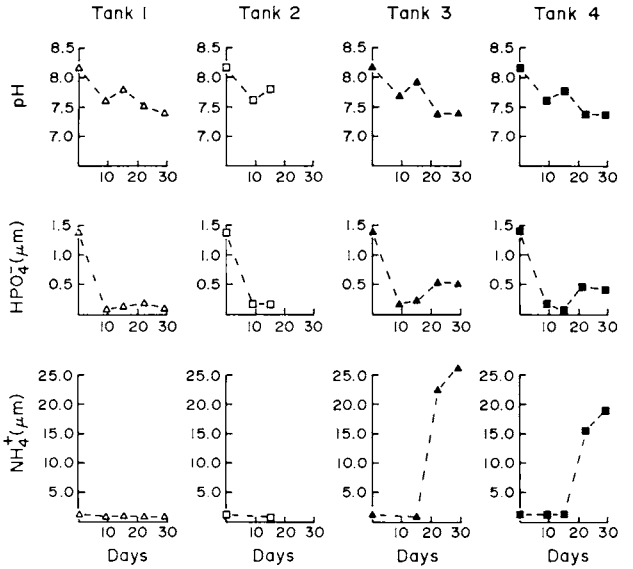

Fig. 10. pH, $HPO_4^=$, NH_4^+ concentrations in overlying water in tank used in *Clymenella* experiment. *Clymenella* added after 15 days to tanks 3 and 4.

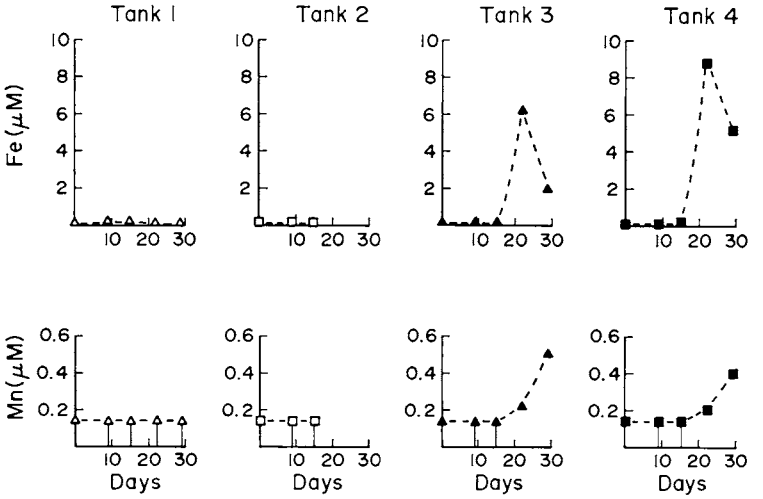

Fig. 11. Fe and Mn concentrations in overlying water in tanks 1, 2, 3, and 4. *Clymenella* added after 15 days to tank 3 and 4.

TABLE 5

Solubility products at 25°C and 1 atm for selected compounds

Reaction	Solubility product	Reference
$Mn_3(PO_4)_2 \cdot 3H_2O \rightleftarrows 3Mn^{++} + 2PO_4^{\equiv} + 3H_2O$	$10^{-34.6}$	(1)
$Fe_3(PO_4)_2 \cdot 8H_2O \rightleftarrows 3Fe^{++} + 2PO_4^{\equiv} + 8H_2O$	$10^{-36.0}$	(2)
$FeS_{\text{mackinawite}} \rightleftarrows Fe^{++} + S^{=}$	$10^{-17.5}$	(3)
$Fe_3S_4 \rightleftarrows 3Fe^{++} + 3S^{=} + S^{o}$	$10^{-18.2}$	(3)
$FeS_{\text{amorphous}} \rightleftarrows Fe^{++} + S^{=}$	$10^{-16.9}$	(3)
$MnS_{\text{alabandite}} \rightleftarrows Mn^{++} + S^{=}$	$10^{-17.8}$	(4)
$MnS_{2\,\text{hauerite}} \rightleftarrows Mn^{++} + S^{=} + S^{o}$	$10^{-20.6}$	(4)
$FeCO_{3\,\text{siderite}} \rightleftarrows Fe^{++} + CO_3^{=}$	$10^{-10.2}$	(5)
$MnCO_{3\,\text{rhodochrosite}} \rightleftarrows Mn^{++} + CO_3^{=}$	$10^{-10.4}$	(6)
$CaCO_{3\,\text{calcite}} \rightleftarrows Ca^{++} + CO_3^{=}$	$10^{-8.42}$	(7)
$CaCO_{3\,\text{aragonite}} \rightleftarrows Ca^{++} + CO_3^{=}$	$10^{-8.25}$	(8)

(1) Nriagu and Dell, 1974 - ΔG_f^o data

(2) Nriagu, 1972

(3) Berner, 1967

(4) Mills, 1974 - ΔG_f^o data

(5) Singer and Stumm, 1970

(6) Morgan, 1967

(7) Jacobsen and Langmuir, 1974

(8) (1.48 x k_{sp} calcite) e.g. Berner, 1976a

Evaluation of equilibrium controls on tank pore water profiles.—Adsorption reactions involving ions such as NH_4^+ and $HPO_4^=$ or the formation of specific solid phases may contribute to the form of the pore water profiles and magnitude of the observed concentrations. The likelihood of equilibrium controls on sediment pore water chemistry in the *Yoldia* tank experiment can be evaluated by calculating the state of saturation with respect to a range of pure solid phases likely to form. The less complete pore water data available for the *Clymenella* experiment do not allow similar determinations in that case.

To calculate dissolved ion activities both nonspecific and specific (ion pairing) effects must be taken into account; techniques for doing this are outlined in detail by Garrels and Christ (1965) and Berner (1971). In the present study, a computer program developed and written by R. Holdren (Holdren, 1977) was used for calculation of activities. Ion pairing for HCO_3^-, $CO_3^=$, $SO_4^=$, $H_2PO_4^-$, $HPO_4^=$, HS^-, OH^-, Cl^-, H^+, Na^+, K^+, Ca^{++}, Mg^{++}, Fe^{++}, and Mn^{++} is calculated using accepted values for association constants at 25°C (for example, Sillén and Martel, 1964; Morgan, 1967), the choices of which are discussed in detail by Holdren (1977). The formation of complexes with organic material is ignored. Activity coefficients are estimated using the extended Debye-Huckel equation for the appropriate ionic concentrations. This results in an error of ~ 10 to 20 percent which becomes insignificant compared to other uncertainties such as the value chosen for the K_{sp} of a given phase.

Charge balances for the data are ± 0.1 percent in the *Yoldia* tank and −0.1 to 0.5 percent in the control assuming Mg/Cl, Na/Cl, and K/Cl ratios of seawater. The calculated γ_T's (total activity coefficient in-

TABLE 6

Yoldia experiment pore water: log (IAP/K) for selected phases

	Reddingite $Mn_3(PO_4)_2 \cdot 3H_2O$		Vivianite $Fe_3(PO_4)_2 \cdot 8H_2O$		Mackinawite FeS		Greigite Fe_3S_4		Alabandite MnS	
Depth	Yoldia	Blank	Yoldia	Blank	Yoldia	Blank	Yoldia	Blank	Yoldia	Blank
0-1	-5.83	-4.62	-7.74	-7.17	-	-	-	-	-	-
1-2	-3.50	-3.09	-4.77	-1.46	-	-	-	-	-	-
2-3	-2.87	-2.59	-4.28	-0.59	-	-	-	-	-	-
3-4	-1.82	-2.09	-4.28	-0.78	-	-	-	-	-	-
4-5	-1.22	-1.24	-3.93	-2.77	-1.4	-2.6	-0.70	-1.9	0.23	-2.9
5-7	-1.12	-0.96	-3.72	-3.09	-0.40	-1.0	0.30	-0.3	1.20	0.46
7-9	-1.11	-0.82	-3.87	-3.20	-0.10	-2.0	0.60	-1.3	-1.6	-0.43

	Rhodochrosite $MnCO_3$		Siderite $FeCO_3$		Calcite $CaCO_3$		Aragonite $CaCO_3$	
Depth	Yoldia	Blank	Yoldia	Blank	Yoldia	Blank	Yoldia	Blank
0-1	-1.27	-0.55	-2.58	-2.06	-0.22	0.26	-0.39	0.087
1-2	-0.73	-0.48	-1.82	-0.60	-0.12	0.021	-0.29	-0.15
2-3	-0.60	-0.43	-1.74	-0.43	-0.078	-0.017	-0.25	-0.19
3-4	-0.43	-0.32	-1.91	-0.55	-0.010	0.023	-0.16	-0.15
4-5	-0.15	-0.093	-1.72	-1.27	0.25	0.20	0.075	0.033
5-7	-0.13	0.038	-1.67	-1.34	0.29	0.35	0.12	0.18
7-9	-0.079	0.11	-1.67	-1.36	0.34	0.49	0.17	0.32

cluding ion pairing) by the model are, for example, 0.16 to 0.17 for Fe^{++}, 0.11 for Mn^{++}, and 0.21 to 0.22 for Ca at tank conditions and are within the expected range (Berner, 1971).

Selected reactions involving some of the solid phases likely to form (see Berner, 1967, 1970; Rickard, 1969; Sholkovitz, 1973; Bray, 1973; Troup, 1974; Norvell, 1974; Holdren, 1977) and a representative K_{sp} for each are given in table 5. Saturation indices (log IAP/K_{sp}) for individual depth intervals are calculated and listed in table 6. Errors in calculation are largest in the cases of phosphate phases where K_{sp}'s are questionable (for example Nriagu, 1972; Nriagu and Dell, 1974; Tessenow, 1974) and in the cases of sulfides where measurement error of pS is probably large. Pure end member phases, particularly for the Fe, Mn-phosphates and carbonates, are unlikely as well. Within this context, several conclusions can be made. (1) Dissolved Fe is controlled by equilibrium with variably stable sulfides below ~4 cm depth in both tanks. (The greigite calculation assumes saturation with respect to elemental sulfur). This is consistent with the black color of the sediment, the known occurrence of Fe-sulfides in NWC sediment (Berner, 1970; Aller, 1977), and the relative stabilities of Fe-sulfides, phosphates, and carbonates in the presence of measurable sulfide. In the control tank, a zone of near saturation with respect to vivianite and siderite occurs just above the sulfide zone, but otherwise Fe concentrations in this near interface region are probably controlled by reaction kinetics and transport as discussed later. (2) Below ~4 cm depth, dissolved Mn is at saturation or supersaturation with respect to several possible solid phases. Because of large uncertainties in the reported K_{sp}'s for Mn-phosphates and sulfides, the formation of these compounds in the tanks cannot be ruled out on the basis of pore water chemistry alone. However, the closest correspondence of calculated IAPs with theoretical solubility is found for $MnCO_3$ This is consistent with the common geologic occurrence of rhodochrosite or solid solutions of Mn, Ca carbonates (for example, Calvert and Price, 1970) and with a number of field studies (Li, Bischoff, and Mathieu, 1969; Holdren, Bricker, and Matisoff, 1975; Holdren, 1977; Aller, 1977). (3) Both calcite and aragonite are undersaturated in selected regions near the sediment-water interface of each tank. Saturation or supersaturation is reached below ~4 cm. Because total alkalinity was used in the calculations, the IAPs tend to be high. Similar saturation states are calculated using the apparent dissociation constants for carbonic acid (Lyman, 1965) and apparent solubilities of calcite and aragonite (Berner, 1976a) in seawater. This gives added confidence to the model used here to determine activities.

Models of transport and kinetic controls.—Simple transport-reaction models can be used together with the equilibrium calculations to help explain similarities and differences in the pore water and solid phase properties of the *Yoldia* and control tanks. Of the pore water constituents that were measured, NH_4^+ is the least reactive in terms of specific phase formation, and its distribution will be considered first in order to substantiate or disprove assumptions about transport and decomposition in

each tank. There is no net sedimentation during the experiment so that, ignoring compaction, the NH_4^+ concentration, C(x,t), in pore water can be described by the one dimensional diffusion-reaction equation (Berner, 1976b):

$$\frac{\partial C}{\partial t} = \frac{D}{1+K}\frac{\partial^2 C}{\partial x^2} + \frac{R_N}{1+K} \tag{2}$$

where:

- t = time
- x = dimension variable, origin at the sediment-water interface, and positive axis into sediment
- K = Langmuir adsorption coefficient for NH_4^+ in linear range
- D = molecular diffusion coefficient modified for tortuosity; assumed constant
- R_N = rate of NH_4^+ production as a function of depth and time

Adsorption is included in the description because NH_4^+ is known to adsorb strongly to organic and clay particles (Mortland and Wolcott, 1965; Nõmmik, 1965). Rosenfeld (1977) has shown that, for marine sediments, adsorption of NH_4^+ is reversible and can be described by Langmuir isotherms. K ranges from ~1 to 2 (Rosenfeld, 1977).

As explained above, because of the homogenization of sediment it will be initially assumed that R_N is constant with depth. Decomposition experiments on sediments from NWC show that R_N is unlikely to be a strong function of time in a closed system over the length of the present experiment as long as temperature is held constant (Aller and Yingst, in preparation). Therefore R_N will be taken as a constant. Deviations from these assumptions will be discussed as they become apparent.

Eq (2) can be solved using the initial and boundary conditions:

A. $t=0$, $C=C_0$, $0 \leq x \leq L$

B. $t>0$, $C=C_T$, $x=0$

C. $\left(\frac{\partial C}{\partial x}\right)_{x=L} = 0$

where:

- L = thickness of sediment to bottom of tank
- C_T = constant overlying water concentration
- C_0 = initial homogenized concentration in sediment

Boundary condition (C) reflects the impermeable lower boundary of the tank. The solution is obtained by a minor modification of the problem solved by Nelson (1952) giving:

$$C = C_T + \frac{R}{2D}x(2L-x) - \frac{16RL^2}{D\pi^3}\sum_{n=1}^{\infty}\frac{e^{-(2n-1)^2\pi^2 Dt/4L^2(1+K)}\sin((2n-1)\pi x/2L)}{(2n-1)^3}$$

$$- \frac{4}{\pi}(C_T - C_0)\sum_{n=1}^{\infty}\frac{e^{-(2n-1)^2\pi^2 Dt/4L^2(1+K)}\sin((2n-1)\pi x/2L)}{(2n-1)} \tag{3}$$

The various constants can be obtained as follows. L = 10 cm as defined and K ~ 1 (Rosenfeld, 1977). The diffusion coefficient for NH_4^+ is estimated by taking the theoretical ratio: $D_{NH_4^+}/D_{SO_4^=}$ at 22°C (from Li and Gregory, 1974) and multiplying it by the $D_{SO_4^=}$ (4×10^{-6}cm²/sec) calculated for Long Island Sound sediment (Goldhaber and others, 1977). This gives a tortuosity corrected $D_{NH_4^+} \sim 7.0 \times 10^{-6}$cm²/sec — in reasonable agreement with laboratory measurements (Rosenfeld, 1977). Charge coupling during diffusion is ignored (Ben Yaakov, 1972).

A minimum R_N can be estimated by using the measured NH_4^+ concentration at 7 to 9 cm, C, compared to the starting value, C_o, to give $R_N/(1+K) \sim (C-C_o)/t$ with t = 45 days. A value of $R_N/(1+K) \sim 7.2 \times 10^{-8}$ mM/sec is obtained. This is a minimum since the mean distance influenced by diffusion in the tank is $x = (2Dt)^{1/2} = 7.4$ cm in 45 days. An independent check comes from decomposition experiments at NWC which gave an average $R_N/(1+K)$ for the upper 10 cm of sediment of $1.8 \pm 0.4 \times 10^{-7}$ mM/sec (22°C) (Aller and Yingst, in preparation). Since the grab sampler used to obtain sediment for the tanks may have captured the upper portion of sediment in a somewhat different proportion than exactly 0 to 10 cm, these R_N values can be considered to be in good agreement.

Using $R_N/(1+K) = 7.2 \times 10^{-8}$ (lower limit), the model generated profile for t = 45 days is given in fig. 12A. The case where $R_N/(1+K) = 8 \times 10^{-8}$ mM/sec is also graphed for even better agreement. Agreement between the observed data and the simple production, adsorption, and transport model is good indicating that the assumptions of the model are reasonable and represent a basically adequate description of the processes affecting NH_4^+ in the tank. Precipitation of NH_4^+ as part of an insoluble phase at depth in the tank would not be illuminated by this treatment of the data. Slight changes in R_N near the interface do not greatly affect the profile, while, as shown below, changes in D do, so that the assumption of constant R_N need really hold only below the

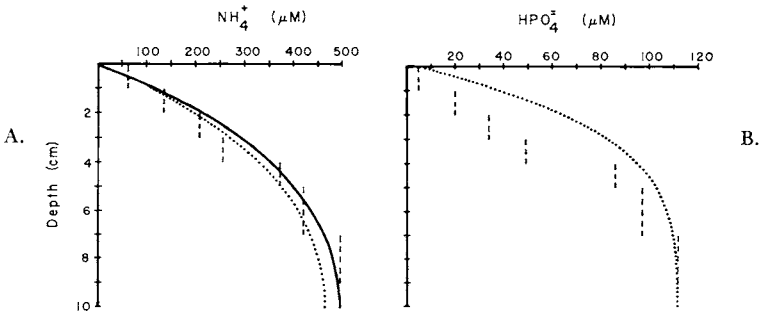

Fig. 12. (A) Single layer, nonsteady-state diffusion-reaction model fit to NH_4^+ pore water profile of *Yoldia* experiment control tank. Control tank data = dashed vertical lines. Model values: $D = 7 \times 10^{-6}$ cm²/sec; R = 12.4 μM/d (14.4×10^{-5} μM/sec, dotted line); R = 13.8 μM/d (16×10^{-5} μM/sec, solid line); K = 1, time = 45 days. (B) Single layer model fit to $HPO_4^=$ pore water profile of control tank. Model values: $D = 2.6 \times 10^{-6}$ cm²/sec; R = 2.08 μM/d (2.4×10^{-5} μM/sec); K = 1; time = 45 days.

upper few centimeters. The model is highly sensitive to values chosen for D and K.

Phosphate data in the control tank were modeled in a similar way, but with $D = 2.6 \times 10^{-6}$ cm²/sec (assume $HPO_4^=$ form, estimate as for $D_{NH_4^+}$) and $R_p/1+K_p = 1.2 \times 10^{-8}$ mM/sec estimated from the concentration change in the 7 to 9 cm interval. No independent estimate of $HPO_4^=$ production other than that obtained from the tank is available. K_p is assumed to be $\sim$ 1 for purposes of the present calculations; at higher K_p's the fit becomes worse. The $HPO_4^=$ data deviate strongly from simple diffusion-production control as shown in figure 12B. The marked upward concavity in the concentration profile presumably results from interaction with Fe, either through precipitation as a distinct phase or irreversible adsorption on oxides (Mortimer, 1941; Carritt and Goodgal, 1954; Li and others, 1972; Syers, Harris, and Armstrong, 1973; Parfitt, Atkinson, and Smart, 1975). The *Yoldia* tank profile shows comparable effects (fig. 3) but is complicated by reworking as discussed below.

It is possible to fit a similar diffusion-production curve to the *Yoldia* tank NH_4^+ data as was done for the control using a slightly higher R_N, but there are several clues that transport-reaction conditions are not the same in the *Yoldia* and control tanks: (1) The flux of Mn out of *Yoldia* tank sediment is three times the control tank during the first 3 days when $(\partial C/\partial x)$ *Yoldia* $\sim$ $(\partial C/\partial x)$ control near the interface must roughly be true (fig. 7; table 2). This means the effective diffusion coefficient for Mn must be at least three times higher near the sediment-water interface in the *Yoldia* tank than control or that Mn production rates differ greatly between tanks. Since the precipitation rate of Mn is pseudofirst order at high reactive-particle concentrations (Lewis, 1976) like that present in the *Yoldia* tank, the discrepancy in flux must be even greater when precipitation is considered. (2) Both the Mn and alkalinity profiles in the *Yoldia* tank are lower in concentration level than the control despite apparently higher rates of organic matter decomposition in the *Yoldia* tank. These higher rates are indicated by slightly higher concentrations of NH_4^+, $HPO_4^=$, HS^-, and ATP in *Yoldia* tank sediment below 4 cm depth (figs. 3 and 4; table 1). (3) The dissolved Fe maximum is greatly lowered in the tank with *Yoldia* compared to the control (fig. 4). (4) The dissolved Ca profiles differ between the tanks in the same way as does Fe.

These differences, as well as similarities between tanks, can be explained by considering the effects of sediment reworking by *Yoldia* on pore water distributions. Two distinctly different kinds of effects can be expected: (1) changes that result from simply altering the rate of transport of fluid and particles in the inhabited zone relative to underlying sediment, and (2) the effects of specific chemical reactions that result when particles are transferred from one diagenetic zone to another during reworking.

Alteration of transport mechanisms by the activities of Yoldia.—The effect of reworking on transport in the *Yoldia* tank sediment can pre-

sumably be described by a composite system where an upper zone has an effective, biogenic diffusion coefficient D_1, and a lower sediment zone is controlled by a molecular diffusion coefficient D_2. Because *Yoldia* is mobile and its activities restricted to a thin zone near the interface, the geometry of diffusion — unlike the case of the sedentary, tube-dweller *Clymenella* (as demonstrated later) — can be adequately incorporated into such an average vertical diffusion coefficient. The use of a diffusion analogue for biogenic reworking and of an average diffusion coefficient in particular assumes that the sample of sediment taken at any given depth integrates over a large enough area (or individual animals) to eliminate heterogeneities in rates and depth of reworking (for example, Hanor and Marshal, 1971; Aller, 1977). Using the same basic form and assumptions as previously, the equations describing this composite system are:

$$\text{Zone 1, } 0 \leq x \leq L_1 \qquad \frac{\partial C_1}{\partial t} = D_1 \frac{\partial^2 C_1}{\partial x^2} + R_1 \tag{4}$$

$$\text{Zone 2, } L_1 \leq x \leq L_2 \qquad \frac{\partial C_2}{\partial t} = D_2 \frac{\partial^2 C_2}{\partial x^2} + R_2 \tag{5}$$

With initial and boundary conditions:

A. $t = 0,\ C = C_0,\ 0 \leq x \leq L_2$

B. $t > 0,\ C = C_T,\ x = 0$

C. $D_1 \left(\frac{\partial C_1}{\partial x}\right) = D_2 \left(\frac{\partial C_2}{\partial x}\right),\ x = L_1$

D. $C_1 = C_2,\ x = L_1$

E. $\frac{\partial C_2}{\partial x} = 0,\ x = L_2$

For simplicity, linear adsorption has been left out at this stage; it may be readily included by dividing both D and R in a given zone by the appropriate factor (1+K). The values of R are constant in each zone but may differ between zones. This allows for more general modeling of the system.

The solution is obtained by method of the Laplace transform and use of the inversion theorem:

Zone 1:

$$C_1 = C_T - \frac{R_1 x^2}{2 D_1} + \frac{R_1 L_1 x}{D_1} + \frac{R_2 x (L_2 - L_1)}{D_1} - \sqrt{\frac{D_2}{D_1}} \sum_{n=1}^{\infty} \left(C_T - C_0 + \frac{R_1}{P_n^2}\right) \cdot \frac{\left(\cos \frac{P_n L_1}{\sqrt{D_1}} \sin \frac{P_n (L_2 - L_1)}{\sqrt{D_2}} \sin \frac{P_n x}{\sqrt{D_1}}\right) e^{-P_n^2 t}}{P_n^2 \Delta'_n} \tag{6}$$

$$- \sum_{n=1}^{\infty} \left(C_T - C_0 + \frac{R_1}{P_n^2} \right) \cdot \frac{\left(\sin \frac{P_n L_1}{\sqrt{D_1}} \cos \frac{P_n (L_2 - L_1)}{\sqrt{D_2}} \sin \frac{P_n x}{\sqrt{D_1}} \right) e^{-P_n^2 t}}{P_n^2 \Delta'_n}$$

$$- (R_2 - R_1) \sqrt{\frac{D_2}{D_1}} \sum_{n=1}^{\infty} \frac{\left(\sin \frac{P_n (L_2 - L_1)}{\sqrt{D_2}} \sin \frac{P_n x}{\sqrt{D_1}} \right) e^{-P_n^2 t}}{P_n^4 \Delta'_n}$$

Zone 2: (7)

$$C_2 = C_T - \frac{R_2 (x - L_2)^2}{2 D_2} + \frac{R_2 L_1 (L_2 - L_1)}{D_1} + \frac{R_2 (L_2 - L_1)^2}{2 D_2} + \frac{R_1 L_1^2}{2 D_1}$$

$$- \sum_{n=1}^{\infty} \left(C_T - C_0 + \frac{R_1}{P_n^2} \right) \frac{\left(\cos \frac{P_n}{\sqrt{D_2}} (x - L_2) \right) e^{-P_n^2 t}}{P_n^2 \Delta'_n}$$

$$- (R_2 - R_1) \sum_{n=1}^{\infty} \frac{\left(\cos \frac{P_n L_1}{\sqrt{D_1}} \cos \frac{P_n}{\sqrt{D_2}} (x - L_2) \right) e^{-P_n^2 t}}{P_n^4 \Delta'_n}$$

Where P_n satisfy and are the n roots of:

$$\sqrt{\frac{D_2}{D_1}} \tan \left(\frac{P_n L_1}{\sqrt{D_1}} \right) = \cot \left(\frac{P_n}{\sqrt{D_2}} (L_2 - L_1) \right) \tag{8}$$

and Δ'_n is defined by:

$$\Delta'_n = \left(\frac{1}{2} \frac{\sqrt{D_2} L_1}{D_1 P_n} + \frac{1}{2} \frac{(L_2 - L_1)}{\sqrt{D_2} P_n} \right) \cos \frac{P_n L_1}{\sqrt{D_1}} \sin \frac{P_n (L_2 - L_1)}{\sqrt{D_2}}$$

$$+ \left(\frac{1}{2} \frac{(L_2 - L_1)}{\sqrt{D_1} P_n} + \frac{1}{2} \frac{L_1}{\sqrt{D_1} P_n} \right) \sin \frac{P_n L_1}{\sqrt{D_1}} \cos \left(\frac{P_n (L_2 - L_1)}{\sqrt{D_2}} \right) \tag{9}$$

The steady state part of the solution has been separated and placed first in the equations. At a time of 45 days only the first two to three terms are needed for convergence of each series; in general, three terms were used in the calculations presented here.

Pore water profiles in the *Yoldia* tank will be considered first. Reasonable limits on the values of the various constants will be initially estimated and then allowed to vary, if necessary, to obtain a better correspondence between measured and modeled distributions. Based on the size of the *Yoldia* present, the depth of the upper zone, L_1, lies between 3 to 4 cm. L_1 is taken to be the minimum 3 cm. The ratio D_1/D_2 can

be estimated using the flux continuity condition (C) above and a linear approximation to the concentration gradients around L_1. The NH_4^+ profile predicts $D_1/D_2 \sim 1.7$, while the alkalinity profile (assumed present as HCO_3^-) predicts $D_1/D_2 \sim 3.1$. (In the upper zone, concentrations were assigned to the midpoint of the sample intervals at 1.5 and 2.5 cm and a line calculated to a depth of 3 cm; in the lower zone the concentrations at 3.5 and 4.5 cm were used). Taking D_2 for HCO_3^- as 3×10^{-6} cm²/sec and for NH_4^+ as 7×10^{-6} cm²/sec, an average $D_1 \sim 1 \times 10^{-5}$ cm²/sec is calculated.

An additional constraint can be placed on the value of D_1 based on the initial flux of Mn from the *Yoldia* tank. This assumes that the production rate of Mn is not different at that stage of the experiment. If the molecular $D_{Mn} = 2.4 \times 10^{-6}$ cm²/sec (estimated as previously for $D_{NH_4^+}$, then $D_1 > 7.2 \times 10^{-6}$ cm²/sec.

Before fitting the data by use of eqs 6 to 9, the behavior of the composite system in general will be examined. The effect of variation in D_1/D_2 is illustrated for the steady state case in figure 13A. Similar results for slightly different composite systems have been presented by Vanderborght, Wollast, and Billen (1977) and Hammond, Simpson, and Mathieu (1975). It is obvious that even with biogenic mixing, reworking will not noticeably affect transport of that ion if $D_1 \sim D_2$, but if $D_1 > D_2$, the concentration is lowered throughout the sediment column. The greater the disparity between D_1 and D_2 for a given ion, other things equal, the greater the effect of reworking on its entire profile. For example, NH_4^+ has a $D_2 \sim 7 \times 10^{-6}$ cm²/sec, so that changes in its profile due to a mixed zone of $D_1 \sim 1 \times 10^{-5}$ should be subtle. D_1/D_2 for HCO_3^- in

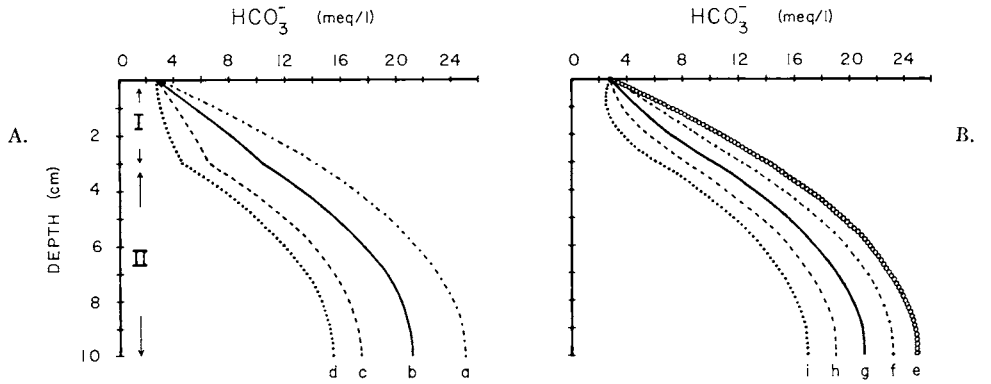

Fig. 13. Composite layer, steady state model showing effect of increasing diffusion or reaction rates in a two layer system. $L_1 = 3$ cm, $L_2 = 10$ cm. (A) $D_2 = 3 \times 10^{-6}$ cm²/sec in all curves, $R_2 = 0.116$ meq/*l*/day (1.34×10^{-6} meq/*l*/ sec) in all curves. Curve a: $D_1 = 3 \times 10^{-6}$ cm²/sec, $R_1 = R_2$. Curve b: $D_1 = 4.5 \times 10^{-6}$ cm²/sec, $R_1 = R_2$. Curve c: $D_1 = 9 \times 10^{-6}$ cm²/sec, $R_1 = R_2$. Curve d: $D_1 = 9 \times 10^{-6}$ cm²/sec, $R_1 = -2R_2$. (B) $D_1 = D_2 = 3 \times 10^{-6}$ cm²/sec in all curves. Curve e: $R_1 = R_2$ (same as curve a). Curve f: $R_1 = 0.1\ R_2 = 0.0116$ meq/*l*/day. Curve g: $R_1 = -R_2 = -0.116$ meq/*l*/day. Curve h: $R_1 = -2R_2$. Curve i: $R_1 = -3R_2$.

the same case is large, and the effect of mixing on its profile should be correspondingly greater. This predicted difference is observed in the data (fig. 3).

Changes in R_1 relative to R_2 do not influence the observed profiles very much as long as L_1 is much less than L_2, and R_1 and R_2 are both positive (fig. 13B). When R_1 becomes negative, that is, the ion under consideration is consumed uniformly in the upper layer, the profile can become significantly affected without any change in diffusion coefficients. In this case, the upper zone profile takes on an increasingly concave shape, like that of the $HPO_4^{=}$ profiles, as R_1 becomes greater than $|-2R_2|$ (fig. 13B). An example where both R_1 and D_1 differ from D_2 and R_2 is given in figure 13A illustrating the effect of increasing D_1 on the shape of the concavity produced by consumption in zone 1. The curves where R_1 is 1/10 R_2 (fig. 13B) and $D_1 = 3/2\ D_2$ (fig. 13A) demonstrate that it is not possible to recognize easily changes in R and D near the interface from the shape of profiles alone, although a significant lowering of concentrations takes place in each instance.

Changing the functional form of R to $R_0e^{-\alpha x}$ through the sediment thickness does not alter the basic conclusions of the composite model. In this case, a break in the concentration profile at the mixing depth is harder to see, but the general lowering of concentration still takes place. The steady state solutions, with the same boundary conditions as above, are:

$$C_1 = C_T - \frac{R_0 x}{D_1 \alpha}\, e^{-\alpha L_2} + \frac{R_0}{D_1 \alpha^2}\,(1 - e^{-\alpha x}) \tag{10}$$

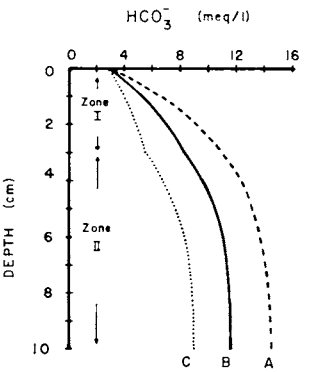

Fig. 14. Composite layer, steady state model showing effect of an exponentially decreasing reaction rate in two layer system rather than constant reaction rates in each zone as in figure 13. $L_1 = 3$ cm, $L_2 = 10$ cm. $R = R_0 \exp(-\alpha x)$, $\alpha = 0.33$; $R_0 = 0.397$ meq/l/day, $\bar{R}$ (0-10 cm) = 0.116 meq/l/day. $D_2 = 3 \times 10^{-6}$ cm²/sec in all curves. Curve A: $D_1 = 3 \times 10^{-6}$ cm²/sec. Curve B: $D_1 = 4.5 \times 10^{-6}$ cm²/sec. Curve C: $D_1 = 9 \times 10^{-6}$ cm²/sec.

$$C_2 = C_T - \frac{R_0 L_1}{D_1\alpha}\, e^{-\alpha L_2} + \frac{R_0}{D_1\alpha^2}\,(1 - e^{-\alpha L_1}) + \frac{R_0}{D_2\alpha}\, e^{-\alpha L_2}\,(L_1 - x) + \frac{R_0}{D_2\alpha^2}\,(e^{-\alpha L_1} - e^{-\alpha x}), \tag{11}$$

and solutions have been graphed for the case where $\alpha = 0.33$, as found normally for rates of sulfate reduction at NWC (Aller and Yingst, in preparation), with R_0 evaluated so that the average R over 10 cm is equivalent to the constant R_2 used in the previous examples (fig. 14). The significance of the depth dependence of R in controlling the final concentrations obtained is illustrated by comparison of the two examples with R = constant and $R = R_0 e^{-\alpha x}$ (figs. 13 and 14).

The transient state solutions for the composite system (eqs 4-9) are applied directly to the *Yoldia* tank NH_4^+, $HPO_4^=$, and HCO_3^- (alkalinity) data in figure 15. The values obtained at best fit are reasonable

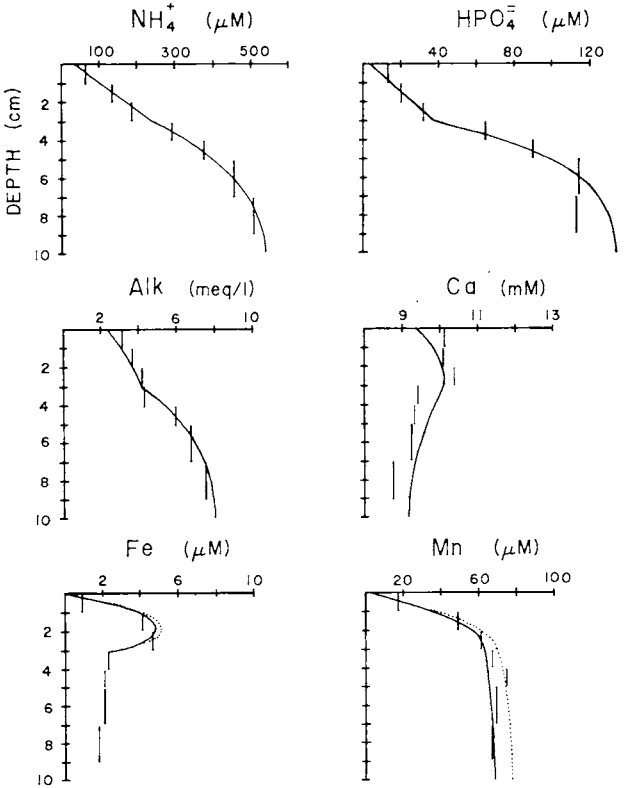

Fig. 15. Composite layer, nonsteady state model fits to *Yoldia* tank data. Values are given in table 7. Alkalinity has been treated as though present entirely as HCO_3^-. Dotted line plot for Fe represents change in assumed lower boundary depth.

within the limits discussed earlier. Adsorption constants of $K \sim 1$ are assumed for both NH_4^+ and $HPO_4^=$. The values of D_1, D_2, R_1, and R_2 are listed in table 7. Model fits to control tank data are also shown (fig. 16). In the case of the control tank $D_1 = D_2$ has been assumed, although porosity changes near the interface may result in slight increases in D_1. It is clear from the previous considerations and from concavities in the $HPO_4^=$ and alkalinity ($\sim HCO_3^-$) profiles that generally $R_1 \neq R_2$. It is also clear that R_1 is not constant with depth, but for simplicity constancy will be assumed. Average consumption rates ($R_1 < 0$) for both $HPO_4^=$ and HCO_3^- were estimated by curve fitting as shown. $L_1 =$ 3 to 4 cm was chosen as a reaction boundary in the controls based on the form of the several profiles. NH_4^+ also appears to be consumed near the interface in both tanks, due probably to nitrification, so that $R_1 < R_2$ results in an even better fit in the control than previously found for the single layer model (figs. 12, 16). $HPO_4^=$ is apparently precipitated in basal sections of the *Yoldia* tank.

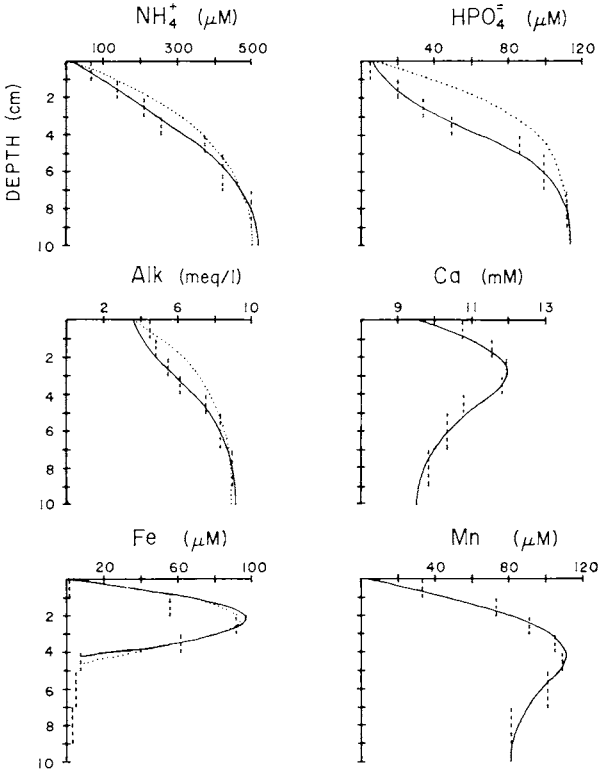

Fig. 16. Composite layer, nonsteady state model fits to control tank data of *Yoldia* experiment. Values are given in table 7. Alkalinity has been treated as entirely HCO_3^-. Dotted lines in the NH_4^+, $HPO_4^=$, and Alk plots represent single layer model predictions. Dotted line plot for Fe represents change in assumed lower boundary depth.

Several important conclusions can be drawn from the composite layer modeling of NH_4^+, $HPO_4^=$, and HCO_3^- pore water profiles. (1) The effect of biogenic reworking by mobile deposit feeders on pore water distributions can be represented in part by an effective diffusion coefficient acting over a fixed depth. In this case a value of $\sim 1 \times 10^{-5}$ cm²/sec was found. (2) Different pore water constituents may be affected to a greater or lesser degree depending on D_1/D_2. (3) Control tank profiles demonstrate that consumption of HCO_3^-, $HPO_4^=$, and apparently NH_4^+ takes place in the upper few centimeters. Alkalinity is probably titrated during sulfide oxidation (see below), $HPO_4^=$ presumably reacts with Fe-oxides, and NH_4^+ may be consumed during nitrification. (4) The modeling demonstrates that in the case of NH_4^+ and $HPO_4^=$, slightly higher net production rates occur at depth in the sediment in the presence of *Yoldia* than in its absence. This is consistent with the higher ATP values found at depth in the *Yoldia* than control tanks. Higher production rates are masked in pore water concentrations by the transport effects of *Yoldia*, adsorption, and possibly precipitation reactions. Higher net production rates for $HPO_4^=$ and HCO_3^- are also found in the upper few centimeters of the *Yoldia* than in the control tank, demonstrating either increases in certain kinds of metabolic activity in the presence of *Yoldia* or decreased relative rates of abiogenic reactions such as $HPO_4^=$ adsorption (figs. 15, 16; table 7). A lower net NH_4^+ produc-

TABLE 7

Model values for figures 15 and 16

Yoldia tank constituent	L_1 (cm)	L_2 (cm)	D_1 (10^{-6}cm²/sec)	D_2 (10^{-6}cm²/sec)	R_1 (μM/day)	R_2 (μM/day)	K
NH_4^+	3	10	10	7	2	16.6	1
$HPO_4^=$	3	10	10	2.6	0.2	3.1	1
Alk-HCO_3^-	3	10	10	3	130	100	-
Ca^{++}	3	10	10	3	180	0	-
Fe^{++} (solid)	3	10	10	2.4	2.6	-1	-
Fe^{++} (dotted)	3	4	10	2.4	2.6	-3	-
Mn^{++} (solid)	3	10	10	2.4	12	-0.1	-
Mn^{++} (dotted)	3	10	10	2.4	13	0.1	-
Control tank							
NH_4^+ (solid)	4	10	7		4	15.5	1
NH_4^+ (dotted)	4	10	7		13.8	13.8	1
$HPO_4^=$ (solid)	4	10	2.6		-1.4	2.2	1
$HPO_4^=$ (dotted)	4	10	2.6		2.08	2.08	1
Alk-HCO_3^- (solid)	3	10	3		-50	130	-
Alk-HCO_3^- (dotted)	3	10	3		116	116	-
Ca^{++}	4	10	3		180	0	-
Fe^{++} (solid)	4	10	2.4		8.7	-5	-
Fe^{++} (dotted)	4	5	2.4		8.45	-13	-
Mn^{++}	4	10	2.4		2.9	-0.05	-

tion rate in the upper zone of the *Yoldia* tank compared to the control may reflect increased nitrification in the former.

With regard to conclusion (4), stimulation of microbial metabolic activity by macrofauna has been noted in several previous cases (for example, Hargrave, 1970, 1976; Fenchel, 1970; Aller and Yingst, 1978). The reasons given include: high turnover of bacteria due to grazing by macrofauna, stimulation by mucus secretions, formation of favorable habitats such as tube walls or fecal pellets, and the flushing of metabolites from sediment by irrigation activity. In the present case, where metabolic activity or biomass (ATP) is also apparently increased *below the feeding zone*, the most probable effect of macrofauna is to lower the concentration of some inhibiting by-product of metabolic activity by the transport mechanism outlined above or to increase the supply of a depleted nutrient (for example, a low molecular weight organic molecule) available only in overlying water or sediment layer by the same means. The effect would be most pronounced when D_1/D_2 is large (for example, fig. 13A).

Particle reworking and redistribution of organic matter.—When expressed as a vertical diffusion coefficient, the rate of particle transport by *Yoldia* has been shown by dimensional analysis of reworking data (Rhoads, 1963) to be $\sim 2 \times 10^{-6}$ cm²/sec for a feeding depth of 3 cm (after Guinasso and Schink, 1975). This is much lower than the effective biogenic diffusion coefficient of $\sim 1 \times 10^{-5}$ cm²/sec calculated above for pore water. The discrepancy arises for several reasons: (1) *Yoldia* pumps water for respiration into its mantle cavity. Although many shelled animals would be effectively sealed from their environment (the taxonomic effect referred to in the introduction), the relatively low degree of mantle fusion in protobranchs together with the use of labial palps helps to irrigate sediment with respiratory water during feeding. Irrigation rates are volumetrically $\sim$ 100 times greater than particle reworking rates (Aller, 1977), so that even at low efficiency of exchange out of the mantle cavity this will be an effective transport mechanism. Pore water solutes presumably diffuse horizontally into the cavity where respiratory currents advect them into overlying water. (2) *Yoldia* is highly mobile. Burrowing does not result in a great deal of particle transport relative to feeding but does greatly increase the exchange of pore water as will be considered in detail in the case of *Clymenella*. Together, burrowing and irrigation during respiratory pumping can easily account for the increase in the effective vertical diffusion coefficient beyond that accounted for by feeding alone.

One of the effects of redistributing particles during feeding can be demonstrated by the percent organic matter (ignition loss) profiles (fig. 5). Organic matter decreases from the interface to a minimum at 3 to 4 cm in the *Yoldia* tank, then increases sharply, and remains relatively constant below that depth. The increase at the surface presumably results from the selection of small or organic-rich particles relative to ambient sedi-

ment at depth (3-4 cm) and placement of these particles at the interface during defecation.

Based on ATP data (fig. 5), these reworked sediment particles are initially depleted in bacterial populations relative to deeper sediment or are colonized by microbes having a different ATP/C ratio. This ATP depletion in surface relative to slightly deeper sediments is also present in the control tank. Both tanks, therefore, differ from natural, unhomogenized sediment samples where ATP is commonly highest in surface material (Yingst, 1978). This may reflect a true depletion of surface substrate in the aerobic zone of the control (see lowered organic matter values), an *apparent* decrease due to a maximum in microbial activity around the macro redox boundary at 1 to 2 cm, or, in the case of the *Yoldia* tank, a grazing phenomenon. In the latter case, a corresponding minimum in ATP occurs at 3 to 4 cm, where particle extraction during feeding takes place. The maximum ATP in between presumably results from recolonization of particles by bacteria and optimal growth conditions along the macro redox boundary in the sediment. The departure of the ATP profiles in both tanks from the typical exponentially decreasing values found in nature supports the earlier assumption that the distribution of organic matter substrate is a major control on microbial activity and reaction rate distribution in sediments.

The reason for the increase of percent organic matter above the starting value at depth in the sediment of both tanks is unknown. It may result from an inaccurate measure of the starting value.

Effects of reworking on Fe and Ca.—The dissolved Ca and Fe concentration profiles in the control tank demonstrate the production of these ions near the sediment-water interface (fig. 4). Ca^{++} production presumably results from the dissolution of $CaCO_3$ — probably aragonite, the most abundant shell debris (see table 6 for calculation). On the other hand, Fe^{++} formation is related to reduction of Fe-oxides (see Krauskopf, 1957) or possibly oxidation of solid phase sulfides (see Stumm and Morgan, 1970; Bloomfield, 1972) along boundaries (micro or macro) between oxidizing and reducing regions of sediment. Since sulfide oxidizes at a lower Eh than Fe^{++}, oxidation of dissolved sulfide alone will also tend to increase Fe^{++} by mass action influence on the Fe-sulfide reactions of table 5. This would occur over a restricted Eh range. Near the sediment-water interface Fe^{++} decreases rapidly due to diffusion and oxide precipitation, while deeper in the sediment it precipitates as a sulfide (table 6). Because oxidation of sulfide, oxidation of Fe-sulfides, and subsequent precipitation of Fe-oxides cause the production of acid, it seems likely that the lowering of pH, the concavity in the alkalinity profile (consumption), and the dissolution of $CaCO_3$ in the control tank are intimately related to sulfide oxidation.

The rates of these production reactions can be estimated by use of eqs 4 to 9 and the assumptions that production reactions are uniform with depth and restricted to the upper 4 cm of the control tank. Diffusion

coefficients were obtained in the way previously described. In the case of Ca^{++}, a good correspondence is found between observed and modeled profiles (figs. 15, 16; table 7). Supersaturation with respect to $CaCO_3$ phases in the lower tank zone (that is, $R_2 = 0$) is consistent with observations in natural sediments (for example, Berner, Scott, and Thomlinson, 1970; see also Ben Yaakov, 1973, table 2 for illustration of this supersaturation phenomenon even after precipitation). No correction for adsorption was made as the model fit becomes worse; a low Ca^{++} adsorption coefficient would be consistent with the low montmorillonite content of Long Island Sound sediments (for example, Rosenfeld, 1977). The observed rate of dissolution could result in the loss of up to ~9 mg $CaCO_3$/g sed/yr from the upper region of the sediment column, assuming 50 percent water content.

The estimated Fe^{++} production rate in the control tank (8.7 μM/d) is less accurate than that for Ca^{++} due to rapid precipitation above and below the major zone of production (fig. 16). The average lower zone precipitation rate (−5 μM/d) was estimated so as to cause the observed decrease in Fe^{++} by a depth of 4 to 5 cm. If precipitation is assumed to take place entirely in the interval 4 to 5 cm (that is, $\partial C/\partial x \sim 0$ at $x = 5$), then the precipitation rate required is −13 μM/d (table 7). This represents an upper limit to the required rate. It should be kept in mind that beneath approx 5 cm depth, equilibrium, not kinetic, controls apparently dominate. Because of the large error in the rate estimates, no attempt was made to correct for adsorption. The calculated Fe^{++} production and precipitation rates are not unreasonably large with respect to the sulfide available for precipitation as shown by sulfide production rates. The average sulfate reduction rate for the sediment column, estimated from the $SO_4^=$ pore water profiles, is 31 μM/d.

In contrast to the control tank, there is only minor evidence of Ca^{++} or Fe^{++} production near the sediment-water interface of the tank containing *Yoldia*. There are several ways in which reworking could result in altered profiles. These relate both to changing the relative rates of processes as well as the location of reactions in the sediment. (1) The increased effective diffusion rate could prevent buildup of reaction products into distinct easily-detected concentration maxima. In fact, if the production rates determined for the control tank are applied to the mixed zone of the *Yoldia* tank ($L_1 = 3$ cm, $D_1 = 1 \times 10^{-5}$), the composite model (eqs 4-9) predicts the observed Ca^{++} profile fairly well (fig. 15; table 7) and the Fe profile with an additional minor decrease in reaction rate (table 7). (Lower zone precipitation rates were estimated in a similar way to the control (table 7)). Much of the difference in Ca and Fe^{++} profiles between the tanks can therefore be accounted for simply by increased transport. (2) During feeding, *Yoldia* places reduced material obtained at depth onto the sediment-water interface. An increased proportion of the sulfide oxidation occurring in the upper 3 to 4 cm of sediment now takes place at the interface where reaction products

from oxidation or dissolution do not build up in pore water because of diffusive loss. Once oxidized at the surface, particles are subducted downward but with a critical change, their surfaces are oxidized so that further oxidation of interior sulfides is lowered, and acid production below the interface minimized. (3) The resulting higher pH of pore water in the upper 4 cm and perhaps higher dissolved O_2 concentrations should greatly increase the precipitation rate of dissolved Fe^{++}. This would lower the observed concentration of Fe^{++} further unless a corresponding increase in production rate occurred. (4) Shell formation and acid excretion by *Yoldia* may act to deplete Ca^{++} and HCO_3^- from both interstitial and overlying water. Although HCO_3^- does show lowered values from those of the control, no depletion in Ca^{++} is evident. This suggests that processes in addition to shell formation are acting to maintain lowered alkalinity. This presumably is related to sulfide oxidation as previously described.

These considerations demonstrate (as did the earlier modeling), that, although reactions may be as or possibly more rapid in the *Yoldia* tank than in the control tank, specific and nonspecific effects of reworking can act to mask their presence. Reactions like $CaCO_3$ dissolution in sediment from the *Yoldia* tank must be largely inferred from control tank pore water profiles, knowledge of how *Yoldia* reworks sediment, changes in overlying water chemistry, or separate experiments such as determining the effect of sulfide oxidation on alkalinity (for example, Aller, 1977). In nature, seasonal temperature cycles can be used to separate temporally such biogenic from abiogenic effects. For example, cores taken during winter periods (2°C) in Long Island Sound have Ca^{++} and Fe^{++} profiles similar to those found in the control tank of the *Yoldia* experiment. Cores taken during the fall, when macrofaunal activity is the highest of the year, show Ca^{++} and Fe^{++} profiles like those of the *Yoldia* tank (Aller, 1977).

Effects of reworking on Mn.—The relatively simple change in transport regimes brought about by *Yoldia* has important effects on dissolved and solid phase Mn distributions. These will now be considered.

Like Fe^{++}, Mn^{++} is produced in sediment by the reduction of Mn-oxides (Krauskopf, 1957), but, unlike Fe, oxidation of a reduced phase is unlikely also to play a role. There is considerable evidence that Mn reduction is metabolically linked to the decomposition of organic matter (Mann and Quastel, 1946; Trimble and Ehrlich, 1968; Bromfield and David, 1976). In field studies, for example, Mn production tracks nutrient elements such as NH_4^+ (Aller, 1977; Holdren, 1977). Production of Mn^{++}, like that of a remineralized nutrient, may therefore be related to the quality of organic matter.

In the present case, it will be assumed that, initially (like NH_4^+), Mn is produced at a constant rate R_{Mn} with depth in tank sediment and that it is subject to the same kind of initial and boundary conditions as described in eqs 4 to 9. Because it was shown earlier that Mn becomes

saturated with respect to a number of solid phases below 4 cm, at some point after the start of the experiment Mn concentration reaches a level at depth where precipitation as a reduced phase becomes likely. For illustrative purposes this phase will be taken as rhodochrosite for reasons discussed earlier.

If, for simplicity, a constant pH = 7.4 is assumed, and $\gamma_T = 0.11$ is taken for Mn, then at saturation with respect to $MnCO_3$:

$$C_{Mn} \sim 0.6/C_{Alk},$$

where C_{Mn} = total concentration of Mn and C_{Alk} = total alkalinity, assumed to be $HCO_3^- + CO_3^=$ only. Using this relation and the composite layer model (eqs 4-9) it is possible to produce a time series of Mn concentration curves in each tank. Both Mn and alkalinity are allowed to increase with time in accordance with the transport-reaction conditions described by eqs 4 to 9. Depending on the values chosen for D and R, at some time and depth in the sediment after the beginning of the experiment, saturation with respect to $MnCO_3$ takes place. At this time, C_{Mn} becomes controlled by the equilibrium condition for rhodochrosite at and below that depth (or a constant supersaturation due to kinetic constraints on precipitation (for example, Holdren, 1977)). Because of its much greater abundance than C_{Mn}, C_{Alk} continues to increase throughout the sediment column according to the kinetic model. Above the depth where saturation is met, Mn concentration is still described by the kinetic model as well, but now the lower boundary L_2 ($\partial C_{Mn}/\partial x = 0$) is determined by where equilibrium control begins and becomes a function of time.

For illustration of the equilibrium-kinetic model, only the control tank will be considered quantitatively. Qualitative conclusions regarding the *Yoldia* tank can be made readily based on the previous models. D_{Mn} and $D_{HCO_3^-}$ (HCO_3^- is assumed dominant for transport modeling) are estimated as done previously. R_{Mn} near the interface of each tank was determined by fitting the kinetic model (eqs 4-9) to the concentration gradients in each case (fig. 16; table 7).

Using the values $R_{Mn} = 2.9$ μM/d; $R_{Alk} = -0.05$ meq/l/d, $0 \leq x \leq 3$; and $R_{Alk} = 0.13$ meq/l/d, $3 \leq x \leq 10$ cm, a hypothetical time series of Mn concentration profiles in the control sediment was generated and is shown in figure 17. The time dependence of L_2 for Mn is not a serious problem because of the relatively rapid attainment of a near constant concentration gradient in the upper few centimeters which is fairly independent of the L_2 values used. The basic features of the final Mn profile at time of sampling the control tank are well described except that the Mn maximum is at a lower depth and of somewhat higher magnitude in the real case. This discrepancy is due in part to assuming a constant pH throughout the tank in the model. The average rate of precipitation of Mn required to sustain the Mn maximum is ~ -0.05 μM/d as shown by direct application of the kinetic model (fig. 16, table 4). The advantage of the composite kinetic-equilibrium model is that it probably reflects

more realistically the successive changes in Mn profiles than a simple application of the time independent kinetic model; that is, $R_2 = 0.05$ μM/d throughout the experiment.

The maximum in the dissolved Mn profile requires diffusion of Mn both toward the interface and toward the tank bottom. This predicts a redistribution of solid phase Mn (see, for example, Holdren, 1977), a prediction substantiated by the measured solid phase Mn levels (fig. 6). The time series of Mn pore water profiles suggests that a maximum appeared only after a few weeks and that because of the nature of the production distribution and the relative rates of Mn and alkalinity production, once formed, the maximum Mn concentration rose rapidly from the tank bottom to a depth of 4 to 5 cm in just a few days. Ignoring other reactions, the maximum theoretically would rise to a depth where production rate is balanced by diffusive loss to the overlying water.

The flux of dissolved Mn to any part of the tank is determined by $\partial C/\partial x$ of the profile at a given time and depth; the modeled gradient can be seen in figures 16 and 17 to decrease exponentially below the pore water maximum. This predicts that most downward diffusing Mn will be precipitated just below the maximum rather than at the tank bottom, a prediction borne out by the solid phase distribution that shows the lower solid phase Mn maximum occurring above the tank bottom (fig. 6).

Sediment reworking by *Yoldia* affects this pattern of Mn redistribution in several ways. Because biogenic diffusion induced by *Yoldia* is greater than D_{Mn} or $D_{HCO_3^-}$, the concentrations of both components are lowered in pore water as demonstrated previously. This means that the dissolved Mn concentration maximum will appear at the tank bottom

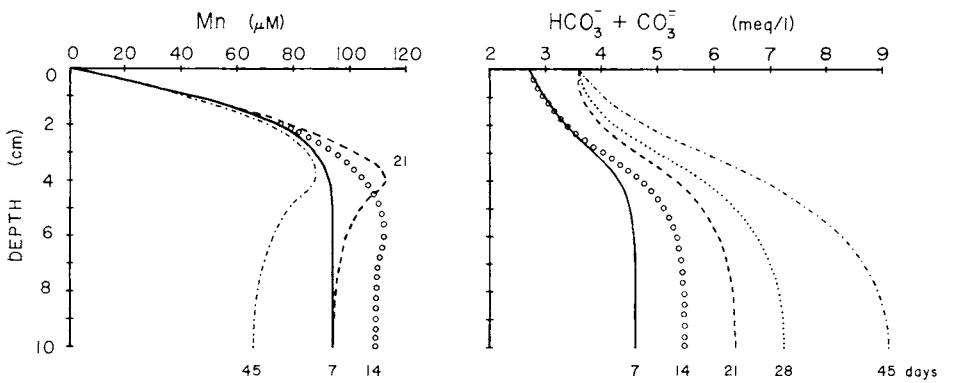

Fig. 17. Nonsteady state-equilibrium composite model showing hypothetical sequence of pore water Mn and alkalinity profiles (assumed to behave as HCO_3^-) which may have occurred through time in the tanks. See text for detailed explanation. Upper boundary value for alkalinity is changed after 14 days from the average for the first 14 days to the average value over time of experiment. $L_1 = 3$ cm, $L_2 = 10$ cm. $D_{Mn} = 2.4 \times 10^{-6}$, $D_{HCO_3^-} = 3 \times 10^{-6}$ cm^2/sec. $R_{Mn} = 2.9$ μM/day. R_1 (HCO_3^-) $= -0.50$ meq/l/day; R_2 (HCO_3^-) $= 0.130$ meq/l/day. The starting values are $C_{Mn} = 73.5$ μM and $C_{Alk} = 3.72$ meq/l. The appropriate times are indicated in the figure.

later in time and that it will reside at a lower depth in the tank longer than in the control before rising to a higher level such as 4 to 5 cm. The result is that the solid phase Mn maximum should occur lower in the *Yoldia* tank than in the control, and, in fact, it does (fig. 6).

Although the assumption of constant R_{Mn} with depth explains many of the features of the present experiments, it is clear that the R_{Mn} values of 2.9 and 12 to 13 μM/d (table 7), chosen for the control and *Yoldia* tanks respectively, are minima. This can be shown by considering the sediment interval 1 to 2 cm, where Mn concentrations dropped by 28 μg/g and 79 μg/g relative to starting values in the control and *Yoldia* tanks during the experiment. This drop predicts an R_{Mn} of 11 to 20 μM/day for that interval, using the appropriate water contents for calculation (table 1). The discrepancy between the estimate of R_{Mn} from pore water and solid phase Mn profiles may result for several reasons: (1) The pore water gradient near the interface is not described adequately by the equations used. (2) The second centimeter interval may have a uniquely high R_{Mn} resulting from the particular conditions, either microbial or physical, that exist there. (3) R_{Mn} may be a strong function of time. In any case, *the presence of Yoldia apparently results in a higher rate of dissolved Mn production than when it is absent.* This is substantiated by both the solid phase measurements and pore water models (figs. 6, 15; table 7).

The rapid redistribution of solid phase Mn during the 45 day period of these laboratory experiments is consistent with field observations where, based on ^{234}Th ($t_{1/2}$ = 24.1 d) time scales (Aller and Cochran, 1976), it was shown that Mn profiles must form and reform on time scales of the order of ~ 35 days (Aller, 1977).

Reworking increases the flux of Mn out of the *Yoldia* tank as discussed previously. Because the overlying water was changed repeatedly, Mn was removed from the system. The higher flux and higher suspended particle concentration onto which precipitation took place in the *Yoldia* tank resulted in a higher loss of Mn during water changes than in the control. This explains the general lowering of Mn levels in the solid phase of the *Yoldia* tank compared to the control (fig. 6). More importantly, it suggests that under natural conditions, *Yoldia* may help maintain a higher proportion of sedimentary Mn in the overlying water than would occur in its absence.

The effect of a tube-dweller on pore water distributions.—As in the case of *Yoldia*, the experiment with *Clymenella* showed that the activities of this organism have a major influence on interstitial and overlying water chemistry (figs. 8-11). *Clymenella* did not feed during the experiment, as evidenced by the lack of fecal mound formation, so that the changes produced by these animals resulted strictly from burrow construction, fluid transport associated with irrigation activity, excretion, and alteration of microbial populations in the sediment rather than particle transport during feeding. This means that although the experi-

ment does not document fully the influence of *Clymenella*, it does allow separation of fluid from particle transport effects on Fe and Mn. It also allows comparison of the processes involved with those associated with *Yoldia*.

Direct excretion of Fe and Mn by *Clymenella* is unlikely to be a source of these metals for overlying or interstitial water (Aller, 1977). Based on the control tank profiles, it also seems unlikely that microbial activity alone can account for the pore water changes observed. The interpretation accepted here is that the changes in Fe^{++} and Mn^{++} distributions produced by *Clymenella* are caused predominantly by tube construction and irrigation.

Mangum (1964) showed that individual *Clymenella* pump from 50 to 100 ml of seawater/animal/day into and out of their burrows for respiratory purposes. This rate lies well within the range reported for other infaunal deposit feeders (Aller, 1977). It can readily be shown in the laboratory that irrigation results in the oxidation of the sandy sediment surrounding tubes inhabited by *Clymenella* (for example, Rhoads, 1967). Oxidation to a maximum distance of a few centimeters away from stationary animals can take place in a period of days depending on grain size and the organic content of the surrounding sediment. Together, tube construction and burrow irrigation offer a transport mechanism which, in some cases, could result in considerable exchange of pore water and overlying water *with a minimum of particle movement.*

A simple mass balance calculation can be made in the *Clymenella* tanks to demonstrate: (1) that the observed increase in Fe and Mn in overlying water can be accounted for by pore water supply consistent with simple exchange by irrigation, and (2) differences between Fe and Mn behavior can be explained by differences in precipitation kinetics during oxygenation.

A minimum loss of Fe and Mn from pore water in the *Clymenella* inhabited tank compared to the controls can be estimated as follows. The pore water concentrations in each depth interval of tank 3 (*Clymenella*) are subtracted from the initial control tank 2 values (table 3). This difference is multiplied by the volume of sediment in each interval (1 l/1 cm interval) and an assumed porosity of 0.5 (reasonable sandy sediment value). The sum of these products over the core length is then taken to obtain a minimum of 5.6 mmoles of Fe and 48μmoles of Mn lost from pore water. This is a minimum, because no production of new Fe and Mn is taken into account.

There are three possible sinks for dissolved Fe and Mn lost from pore water in this system. (1) The introduction of oxygen into pore water by irrigation activity may cause precipitation of Fe or Mn in ambient sediment or at preferred sites such as burrow walls (for example, Aller and Yingst, 1978). (2) If exchange is rapid relative to precipitation rates both dissolved Fe and Mn will be advected out of the sediment body along the tube conduits and into overlying water. (3) Once intro-

duced into overlying water either Fe or Mn can precipitate onto environmental surfaces.

The above possibilities are not exclusive, and the data indicate that each occurs to some extent. Evidence that possibility (1) takes place comes from the changes in Fe/Mn ratios in pore water after the introduction of *Clymenella*. Data in table 3 show that, except for one depth interval (8-9 cm), the Fe/Mn ratio is lowered in the *Clymenella* tank compared to the control. Since there is no reason to believe that Fe would be transported out of sediment preferentially to Mn, this change implies preferential precipitation of Fe relative to Mn during the initial introduction of seawater by irrigation. This difference is consistent with the more rapid precipitation kinetics of Fe relative to Mn in oxygenated waters (Stumm and Lee, 1961; Hem, 1963, 1964; Morgan, 1967). Water advected out of burrows during irrigation therefore had a lower Fe/Mn ratio than inital pore water.

The increase in Fe and Mn in overlying water is proof that (2) occurs. Ignoring precipitation, the minimum quantity of Fe and Mn transferred to overlying water can be calculated by taking the maximum increase in overlying water concentration and multiplying by $\sim 60l$, the quantity of water involved. This gives for tank 3: $\Delta Fe \sim 0.4$ mmoles and $\Delta Mn \sim 22$ μmoles after addition of *Clymenella*; tank 4, for which no pore water profiles are available, has similar increases of: $\Delta Fe \sim 0.5$ mmoles and $\Delta Mn \sim 16$ μmoles. It is then possible to account for ~ 50 percent of the minimum Mn (calculated previously) lost from pore water as standing concentration in overlying water while only ~ 10 percent of the Fe found missing from pore water occurs as standing concentration in overlying water.

There are several types of evidence that possibility (3), precipitation out of overlying water, takes place. The most quantitative is the obvious decrease in Fe concentration with time (fig. 11); this decrease takes place preferentially to Mn so that Fe/Mn ratios drop through time in overlying water. Qualitatively it was observed that in tanks with *Clymenella* an orange-yellow precipitate, soluble in dilute HCl, began to form at the sediment-water interface, around burrow openings, and on tank walls a day or so after introduction of animals, and that this precipitate increased through time. Similar observations have been made for other burrows (for example, Myers, 1973). Generally, no precipitate formed in control tanks, although a similar precipitate would form, if the surface oxidized layer were gently scraped away in a small area. This precipitate is most probably $Fe(O)_x(H_2O)_y$ with various coprecipitates including Mn.

It has been shown to this point that the changes in pore water profiles and overlying water chemistry, which took place after introduction of *Clymenella*, can be consistently explained by irrigation transport and exchange of overlying water with pore water, that material balances between components are reasonable, and that differences in the relative

behavior of Fe and Mn are in accordance with known differences in their properties. It is also possible to put limits on the rate of pore water transport by use of simple diffusion models and to demonstrate that it is not unusually rapid transport when the transport geometry of the system is considered.

Alteration of transport rates by irrigation of permanent burrows.— The distribution of a pore water species, C, in a one dimensional cartesian coordinate system with no compaction or sedimentation is described by eq 2 as previously stated. The minimum, effective diffusion coefficient required to produce the observed pore water changes between *Clymenella* and control tanks can be estimated from that equation as follows. Assume, as before, that the tank sediment can be approximated by a slab of thickness $0 \leq x \leq L$. Let $R = 0$ (to obtain minimum D) and let the initial and boundary conditions be:

A. $t = 0$, $C = mx$
B. $x = L$, $\partial C/\partial x = 0$
C. $x = 0$, $C = 0$, $t > 0$

The initial condition describes a linearly increasing Fe or Mn concentration (slope = m) beneath the sediment-water interface. The solution for C at a given time and position is (modified after Carslaw and Jaeger, 1959, p. 97):

$$C = -\frac{8Lm}{\pi^2} \sum_{n=0}^{\infty} \frac{1}{(2n+1)^2} \cos\left[\frac{(2n+1)\,\pi\,(L-x)}{2L}\right] e^{-D(2n+1)^2\pi^2 t/4L^2} \tag{12}$$

Because Mn behaves more conservatively than Fe (that is, $R < 0$), it will be used in calculation. Ignoring the fact that Mn concentration increases in the top 2 cm after irrigation (discussed below), the question to be answered is: what would D have to be in order to lower Mn concentration in the interval 8 to 9 cm from 29 μM to 1.8 μM in 13 days by vertical diffusion? Calculation shows $D = 2$ to 3×10^{-4} cm^2/sec with $m = 2.3$ μM/cm, $L = 11$ cm (thickness of zone for which data are available). This is a very large diffusion coefficient.

The diffusion coefficient required to accomplish transport can be lowered significantly by more realistically approximating the experimental transport geometry. In the real case the sediment slab is drilled by $\sim$ 30 vertical cylinders (burrows) $\sim$ 10 to 12 cm in length and 0.3 cm diameter. Diffusion occurs horizontally around these cylinders in addition to vertically. In general, the distribution of cylinders (burrows) is not known and is time dependent, although time dependence in position is minimal in the case of sedentary animals. For the sake of illustration a number of additional approximations can be made in order to demonstrate how the required diffusion coefficient changes when a more realistic geometry of diffusion is used. The case of random burrow orientation is treated elsewhere (Aller, 1977).

Assume that *Clymenella* distribute themselves equal distances from their nearest neighbors so that looking down on the sediment the tube openings (30) would be hexagonally packed at the maximum distance possible in the 0.1 m^2 area allowed. Any three tubes now act as the vertices of equilateral triangles the sides of which are 7.9 cm long, so that burrow axes are all 7.9 cm apart from each other. If each burrow (tube) is imagined to be the central axis of a vertically oriented hollow cylinder (annulus of sediment) having inner radius 0.15 cm and outer radius 3.95 cm (half the distance between tube axes) then most of the sediment in the tank can be assigned to one burrow or another; only the center of each triangle of sediment described by any three burrow openings and associated cylindrical shells is unaccounted for and is ignored here. Because all burrows are identical in this arrangement, the transport problem can now be further approximated to the case of diffusion in the wall of a single infinite hollow cylinder with uniform initial concentration C_0 (an approximation), the inner boundary $r_1 = 0.15$ cm of which is held at $C = 0$ by irrigation and at the outer boundary $r_2 = 3.95$ cm the condition $(\partial C/\partial r) = 0$ is required because of intersection with a neighboring cylinder zone (fig. 18). This problem is analagous to transport around a well and is solved for the general case by Muskat (1934, p. 82-85); in this instance the solution is:

$$C(r,t) = -\pi C_0 \sum_{n=1}^{\infty} \frac{J_0(\alpha_n r_1)\, J_1(\alpha_n r_2)\, U(\alpha_n r)\, e^{-D\alpha_n^2 t}}{J_0^2(\alpha_n r_1) - J_1^2(\alpha_n r_2)} \tag{13}$$

α_n = roots of

$$U(\alpha_n r_1) = Y_1(\alpha_n r_2)\, J_0(\alpha_n r_1) - J_1(\alpha_n r_2)\, Y_0(\alpha_n r_1) = 0 \tag{14}$$

where $J_\nu(x)$ and $Y_\nu(x)$ are the appropriate Bessel functions of the first and second kind in standard notation (ν = order). Manipulation of the

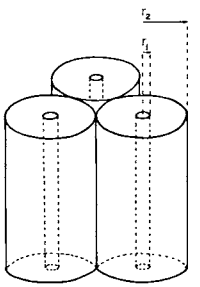

Radial - Hollow Cylinder Model

$$\frac{\partial C}{\partial t} = \frac{D}{r}\left[\frac{\partial}{\partial r} r \frac{\partial C}{\partial r}\right]$$

$t = 0;\ C = C_0,\ r_1 \le r \le r_2$

$t > 0;\ r = r_1, C = 0;\ r = r_2, \frac{\partial C}{\partial r} = 0$

Fig. 18. Idealized diffusion geometry and radial model conditions used to account for pore water concentration changes produced by *Clymenella*.

solution for different D values using the appropriate roots ($\alpha_1 = 0.223$, $\alpha_2 = 0.527$) of the cylinder function ($U(\alpha_n r)$) produces a $D \sim 4.5 \times 10^{-5}$ cm^2/sec required to change the average concentration from ~ 29 μM to ~ 2 μM over the annulus in ~ 13 days. This value is still slightly larger than most molecular diffusion coefficients calculated for sediments (Goldhaber and others, 1977) suggesting that precipitation took place (that is, concentration was lowered by another process in addition to transport, $R<0$), that animals were somewhat mobile thereby increasing the effective number of tubes and decreasing r_2, or that, in sands at least, some advection away from the burrows also occurs during irrigation.

Because of the form of the transport equations and their solution, the diffusion coefficient required to effect a given amount of exchange in sediment by this mechanism will decrease as the factor L^2 (in argument of exponent) decreases where L = half the average distance between burrows. This demonstrates that in natural situations where mixed populations of tube-dwelling species occur and the average distance between burrows may be quite small (fig. 19), the diffusion coefficient required to effect exchange at any given depth will decrease radically from that required by equivalent vertical diffusion. As illustrated in figure 19, which shows natural densities of *Clymenella* and capitellid polychaete tubes at Calves Pasture Point where collections were made, an ion need diffuse only about 0.5 to 1.0 cm horizontally to escape into overlying water, although its vertical distance from the interface is 10 to 15 cm.

The effect of permanent burrows and burrow irrigation can in some ways be viewed as decreasing the net distance to the interface for a diffusing molecule but more generally viewed as changing the geometry of diffusion paths. Unfortunately, permanent dwelling burrows also be-

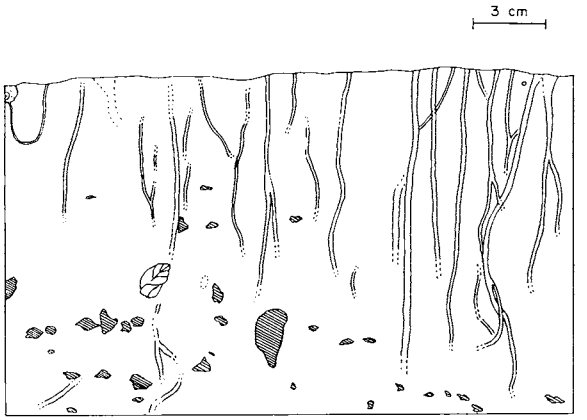

Fig. 19. Tracing of X-radiograph of 2.5 cm thick, vertically oriented slab of sediment which shows natural densities of *Clymenella* and capitellid tubes at Calves Pasture Point, Barnstable Harbor, Mass. (June 29, 1974). Large particles are cross hatched; a gastropod shell is present on left side. Note biogenic graded bedding resulting from selective particle transport during feeding (Rhoads and Stanley, 1965). Some tubes pass in and out of plane of X-radiograph.

come sites of preferential microbial activity and associated diagenetic reactions (Aller and Yingst, 1978) greatly complicating modeling of even the most simple geometries. Tube wall properties may also influence exchange. Where most animals are mobile rather than relatively sedentary like *Clymenella,* their exact spatial distribution becomes less important in controlling transport and the use of vertical diffusion coefficients more appropriate, as discussed previously for *Yoldia.* The two cases, *Clymenella* and *Yoldia,* may be considered end-members in the description of biogenic transport. Both these end-members contribute to transport in nature and, as concepts, grade naturally into one another as animal mobility increases or decreases.

Influence of Yoldia *and* Clymenella *on sediment-overlying water interaction.*—Both tank experiments demonstrated that reworking increases the exchange flux of pore water solutes with overlying water. The *Clymenella* experiment shows increased flux of Fe, Mn, $HPO_4^=$, and NH_4^+ from sediment into overlying water (figs. 10-11). As shown earlier, both the Fe and Mn fluxes can be explained by pore water supply. It is likely that NH_4^+ and $HPO_4^=$ increases are also predominantly from a sediment source. For example, to be supplied by excretion alone, the NH_4^+ flux would require an excretion rate by *Clymenella* of $\sim$ 4 μmoles/worm/day. Typical literature values of NH_4^+ release by polychaetes are 3 to 6 μmoles/g-worm/day by wet weight (Harris, 1959; Hult, 1969; O'Malley and Terwillinger, 1975). *Clymenella torquata* can be expected to have wet weights $\leq$ 0.1 g (see Mangum, 1964) implying that only $\sim$ 10 percent of the observed NH_4^+ flux out of tank sediment can be accounted for by excretion from *Clymenella.* In addition, NH_4^+ need not be conservative in tank water, so that measured fluxes are minima.

Fe and Mn released into overlying water during reworking may reprecipitate onto surface sediment or suspended particles. In doing so, the oxides of these metals can scavenge additional elements from the water column (for example, Aston and Chester, 1975; Turekian, 1977). Such stripping of otherwise soluble elements can be seen in the decrease in overlying water $HPO_4^=$ during Fe precipitation in the *Clymenella* tank (fig. 10). This scavenging process also occurs in the *Yoldia* tank experiment as demonstrated by lower $HPO_4^=$ levels in water overlying sediment in the *Yoldia* tank than in the control (fig. 7; table 2). In this case, the ejection of feces into the water column and reworking of the interface by *Yoldia* increases the turbidity of water overlying the *Yoldia* tank relative to the control (see, for example, Rhoads and Young, 1970). Since the flux of $HPO_4^=$, as illustrated by NH_4^+, should be greater in the *Yoldia* tank due to reworking and excretion, the most reasonable explanation for the observed lowering is scavenging by particles rich with surface Fe-oxides. In addition to Fe, Mn, and P, other elements subject to scavenging by particles should be preferentially removed over natural bottom areas inhabited by these organisms as found for ^{234}Th (Aller and Cochran, 1976; Aller, 1977).

The particles enriched in surface oxides in the above manner fall back to the sediment surface where they undergo reduction. This is illustrated in the *Clymenella* experiment, where Fe and Mn precipitated at the interface after release during irrigation is undergoing remobilization (fig. 8). (A corresponding increase in surface sediment pH occurs during this oxide reduction as shown in fig. 9 (Boström, 1967)). If particles had been reworked by *Clymenella*, the oxide-coated particles would have rapidly dropped deeper into the sediment, the Fe and Mn further remobilized, and then a fraction refluxed back out into overlying water. This sequence of events, complicated by sulfide oxidation, presumably happened in the *Yoldia* tank where feeding did take place. The result of particle reworking and irrigation activities is therefore to increase the rate and magnitude of the sediment-water flux of Fe and Mn and to maintain a supply of highly reactive, freshly oxidized particles at both the sediment-water interface and in overlying water. This maximizes the efficiency of the Fe, Mn-oxide scavenging system.

SUMMARY

1. Two separate sets of experiments were performed in the laboratory in order to study under relatively controlled and simplified conditions the chemical changes produced by deposit-feeding organisms in marine sediment and overlying water. The organisms used, *Clymenella torquata* and *Yoldia limatula*, are representative of two important and distinctive types of deposit feeders. *Clymenella*, a maldanid polychaete, is a relatively sedentary tube-dweller, lives in sediment containing sand, and normally feeds below 10 cm. *Yoldia*, a protobranch bivalve, is highly mobile, lives in muds, and feeds below the surface but in the upper 4 cm.

2. Because of *Yoldia's* mobility and restriction to a zone near the interface, transport of pore water by these animals can be described adequately by a two layer diffusion model in which a biogenic diffusion coefficient of $\sim 1 \times 10^{-5}$ cm^2/sec is effective in the zone of feeding, and the underlying sediment is controlled by molecular diffusion. Biogenic transport changes the concentrations of ions and, under some conditions, the shapes of profiles of ions which have diffusion coefficients less than $\sim 1 \times 10^{-5}$ cm^2/sec in sediment beneath the reworked zone. Particle transport during reworking is at least 10 times slower than the effective rate of pore water transport.

3. Ingestion, digestion, and particle reworking redistributes organic material and contributes to the formation of profiles of organic matter where concentration is relatively high at the interface and falls off with depth.

4. Interstitial water profiles of Fe, Mn, Ca, $HPO_4^=$, alkalinity (assumed present as $\sim HCO_3^-$), and NH_4^+ are altered by reworking in accordance with their individual chemistry and physical properties. Modeling of the pore water or solid phase distributions allows the calculation of average rates of production or consumption of these ions in the general sediment or in selected horizons.

5. Mn is shown to form solid phase concentration profiles similar to natural ones over laboratory time scales of a month. The activities of *Yoldia* increase the rate of dissolved Mn production in restricted intervals of sediment to 2 to 4 times that of the control.

6. Microbial ATP and, in some cases, production or consumption rates of decomposition products are apparently increased in the presence of *Yoldia*. Because these increases can take place away from the actual zone inhabited by *Yoldia*, they probably result as a by-product of changes in the transport of metabolites into or out of sediment as illustrated by models.

7. The construction and irrigation of tubes by *Clymenella* alter the rate and geometry of pore water diffusion in sediment. This results in rapid exchange of pore water constituents such as Fe, Mn, NH_4^+, and $HPO_4^=$ with overlying water. When modeled as a strictly vertical diffusion process, such as in the case of *Yoldia*, a diffusion coefficient of 2 to 3 $\times$ 10^{-4} cm^2/sec is required to produce the observed changes. A horizontal diffusion coefficient of 4.5 $\times$ 10^{-5} cm^2/sec, calculated for an ideal arrangement of tubes, is also capable of explaining the observed changes. The required coefficient becomes lower when the system is described more accurately. In natural bottom sediments, populations of tube dwellers may consist of several kinds of species with relatively closely packed burrows. The horizontal diffusion coefficient required to produce deep vertical exchange of sediment pore waters by irrigation decreases dramatically as the average distance between burrows decreases.

8. Particle reworking and irrigation by both *Yoldia* and *Clymenella* increase the sediment-water flux of Fe and Mn above the rate determined by simple one-dimensional molecular diffusion. These metals precipitate as oxides onto particles in the overlying water, scavenge additional elements such as P from the water, and return to the sediment surface. Continued reworking maintains the Fe, Mn oxide scavenging-reflux system in a fresh, highly reactive state.

ACKNOWLEDGMENTS

Thanks to R. Wells, J. Yingst, W. Ullman, and D. Rhoads for aid in the field over the course of this work. J. Yingst made the ATP determinations. R. Berner, D. Rhoads, and K. Turekian critically read and commented on this work and provided much helpful discussion throughout. V. Barcelon provided advice on the solution of the composite layer model. Computer time was supplied by the University of Chicago. I am grateful for the very helpful reviews given by M. Goldhaber, C. Martens, A. Myers, B. Billen, and J.-P. Vanderborght. Support was provided by ERDA grant Ey-76-S-02-3573 (K. K. Turekian, principal investigator) and NSF grant GA-42-838 (D. C. Rhoads, principal investigator). Support was also provided by an NSF Fellowship.

REFERENCES

Aller, R. C., ms, 1977, The influence of macrobenthos on chemical diagenesis of marine sediments: Ph.D. dissert., Yale Univ., New Haven, Conn., 600 p.

Aller, R. C., and Cochran, J. K., 1976, $^{234}Th/^{238}U$ disequilibrium in nearshore sediment: particle reworking and diagenetic time scales: Earth Planetary Sci. Letters, v. 20, p. 37-50.

Aller, R. C., and Yingst, J. Y., 1978, Biogeochemistry of tube dwellings: A study of the sedentary polychaete *Amphitrite ornata* (Leidy): Jour. Marine Research, v. 36, p. 201-254.

Aston, S. R., and Chester, R., 1973, The influence of suspended particles on the precipitation of iron in natural waters: Estuarine and Coastal Marine Sci., v. 1, p. 225-231.

Ben-Yaakov, S., 1972, Diffusion of seawater ions. I. Diffusion of seawater into a dilute solution: Geochim. et Cosmochim. Acta., v. 36, p. 1395-1406.

———— 1973, pH buffering of pore water of recent anoxic marine sediments: Limnology Oceanography, v. 18, p. 86-94.

Berner, R. A., 1963, Electrode studies of hydrogen sulfide in marine sediments: Geochim. et Cosmochim. Acta, v. 27, p. 563-575.

———— 1967, Thermodynamic stability of sedimentary iron sulfides: Am. Jour. Sci., v. 265, p. 773-785.

———— 1970, Sedimentary pyrite formation: Am. Jour. Sci., v. 268, p. 1-23.

———— 1971, Principles of Chemical Sedimentology: New York, McGraw-Hill, Inc., 240 p.

———— 1976a, The solubility of calcite and aragonite in seawater at atmospheric pressure and 34.5% salinity: Am. Jour. Sci., v. 276, p. 713-730.

———— 1976b, Inclusion of adsorption in the modeling of early diagenesis: Earth Planetary Sci. Letters, v. 29, p. 330-340.

Berner, R. A., Scott, M. R., and Thomlinson, C., 1970, Carbonate alkalinity in the pore waters of anoxic marine sediments: Limnology Oceanography, v. 15, p. 544-549.

Bloomfield, C., 1972, The oxidation of iron sulphides in soils in relation to the formation of acid sulphate soils and of ochre deposits in field drains: Jour. Soil Sci., v. 23, p. 1-16.

Boström, K., 1967, Some pH-controlling redox reactions in natural waters, *in* Equilibrium Concepts in Natural Water Systems: Am. Chem. Soc., Adv. in Chemistry Series, v. 67, p. 286-311.

Bray, J. T., ms, 1973, The behavior of phosphate in the interstitial waters of Chesapeake Bay sediments: Ph.D. dissert., The John Hopkins Univ., Baltimore, Md., 149 p.

Bricker, O. P., and Troup, B. N., 1975, Sediment-water exchange in Chesapeake Bay, *in* Cronin, L. E., ed., Estuarine Research, 1. Chemistry, Biology and the Estuarine System: New York, Academic Press, p. 3-27.

Bromfield, S. M., and David, D. J., 1976, Sorption and oxidation of manganous ions and reduction of manganese oxide by cell suspensions of a manganese oxidizing bacterium: Soil Biology Biochemistry, v. 8, p. 37-43.

Calvert, S. E., and Price, N. B., 1970, Composition of manganese nodules and manganese carbonates from Loch Fyne, Scotland: Contr. Mineralogy Petrology, v. 29, p. 215-233.

Carslaw, H. S., and Jaeger, J. C., 1959, Conduction of Heat in Solids: Oxford, Clarendon Press, 510 p.

Carritt, D. E., and Goodgal, S., 1954, Sorption reactions and some ecological implications: Deep Sea Research, v. 1, p. 224-243.

Christian, R. R., Bancroft, K., and Wiebe, W. J., 1975, Distribution of microbial adenosine triphosphate in salt marsh sediments at Sapelo Island, Georgia: Soil Sci., v. 119, p. 89-97.

Degobbis, D., 1973, On the storage of sea water samples for ammonia determination: Limnology Oceanography, v. 18, p. 146-150.

Fenchel, T., 1970, Studies on the decomposition of organic detritus derived from the turtle grass *Thalassia testudinum*: Limnology Oceanography, v. 15, p. 14-20.

Garrels, R. M., and Christ, C. L., 1965, Solutions, Minerals and Equilibria: New York, Harper and Row Pub. Inc., 450 p.

Gieskes, J. M., and Rogers, W. C., 1973, Alkalinity determination in interstitial waters of marine sediments: Jour. Sed. Pet., v. 43, p. 272-277.

Goldberg, E. D., 1954, Marine geochemistry. I. Chemical scavengers of the sea: Jour. Geology, v. 62, p. 249-265.

Goldhaber, M. B., and Kaplan, I. R., 1974, The sulfur cycle, *in* Goldberg, E. D., ed., The Sea, v. 5, Marine Chemistry: New York, John Wiley & Sons, p. 569-655.

———— 1975, Apparent dissociation constants of hydrogen sulfide in chloride solutions: Marine Chemistry, v. 3, p. 83-104.

Goldhaber, M. B., Aller, R. C., Cochran, J. K., Rosenfeld, J. K., Martens, C. S., and Berner, R. A., 1977, Sulfate reduction diffusion and bioturbation in Long Island Sound sediments: report of the FOAM group: Am. Jour. Sci., v. 277, p. 193-237.

Goto, K., Komatsu, T., and Furukawa, T., 1962, Rapid colorimetric determination of manganese in waters containing iron: Anal. Chim. Acta, v. 27, p. 331-334.

Guinasso, N. L., Jr., and Schink, D. R., 1975, Quantitative estimates of biological mixing rates in abyssal sediments: Jour. Geophys. Research, v. 80, p. 3032-3043.

Hammond, D. E., Simpson, H. J., and Mathieu, G., 1975, Methane and Radon-222 as tracers for mechanisms of exchange across the sediment-water interface in the Hudson River Estuary, *in* Church, T. M., ed., Marine Chemistry in the Coastal Environment: Am. Chem. Soc., Symposium ser. 18, p. 119-132.

Hanor, J. S., and Marshal, N. T., 1971, Mixing of sediment by organisms, *in* Perkins, B. F., ed., Trace fossils: Louisiana State Univ. Misc. Pub. 71-1, p. 127-136.

Hargrave, B. T., 1970, The effect of a deposit-feeding amphipod on the metabolism of benthic microflora: Limnology Oceanography, v. 15, p. 21-30.

———— 1976, The central role of invertebrate faeces in sediment decomposition, *in* Anderson, J. M., and Macfadyen, A., eds., The Role of Terrestrial and Aquatic Organisms in Decomposition Processes: British Ecol. Soc. Symposium, 17th, p. 285-299.

Harris, E., 1959, The nitrogen cycle in Long Island Sound: Bingham Oceanog. Colln. Bull., v. 17, p. 31-65.

Hem, J. D., 1963, Chemical equilibria and rates of manganese oxidation: U.S. Geol. Survey Water-Supply Paper 1667-A, 64 p.

———— 1964, Deposition and solution of manganese oxides: U.S. Geol. Survey Water-Supply Paper 1667-B, 42 p.

Holdren, G. R., Jr., ms, 1977, Distribution and behavior of manganese in the interstitial waters of Chesapeake Bay sediments during early diagenesis: Ph.D. dissert., The John Hopkins Univ., Baltimore, Md., 191 p.

Holdren, G. R., Jr., Bricker, O. P., and Matisoff, G., 1975, A model for the control of dissolved manganese in the interstitial waters of Chesapeake Bay, *in* Church, T. M., ed., Marine Chemistry in the Coastal Environment: Am. Chem. Soc., Symposium ser. 18, p. 364-381.

Hult, J. E., 1969, Nitrogenous waste products and excretory enzymes in the marine polychaete *Cirriformis spirobranchia* (Moore): Comparative Biochemistry Physiology, v. 31, p. 15-24.

Jacobson, E. L., and Langmuir, D., 1974, Dissociation constants of calcite and $CaHCO_3^+$ from 0 to 50°C: Geochim. et Cosmochim. Acta, v. 38, p. 301-318.

Jenne, E. A., 1968, Controls on Mn, Fe, Co, Ni, Cu, and Zn concentrations in soils and water: significant role of hydrous Mn and Fe oxides; Trace Inorganics in Water: Am. Chem. Soc., Adv. Chemistry Series, v. 73, p. 337-387.

Kalil, E. K., and Goldhaber, M., 1973, A sediment squeezer for removal of pore waters without air contact: Jour. Sed. Pet., v. 43, p. 553-557.

Kester, D. R., and Pytkowicz, R. M., 1967, Determination of the apparent dissociation constants of phosphoric acid in seawater: Limnology Oceanography, v. 12, p. 243-252.

Krauskopf, K. B., 1956, Factors controlling the concentration of thirteen rare metals in seawater: Geochim. et Cosmochim. Acta, v. 9, p. 1-32.

———— 1957, Separation of manganese from iron in sedimentary processes: Geochim. et Cosmochim. Acta, v. 12, p. 61-84.

Levinton, J. S., and Bambach, R. K., 1975, A comparative study of Silurian and recent deposit-feeding bivalve communities: Paleobiology, v. 1, p. 97-124.

Lewis, D. M., ms, 1976, The geochemistry of manganese, iron, uranium, lead-210, and major ions in the Susquehanna River: Ph.D. dissert., Yale Univ., New Haven, Conn., 272 p.

Li, W. C., Armstrong, D. E., Williams, J. D. H., Harris, R. F., and Syers, J. K., 1972, Rate and extent of inorganic phosphate exchange in lake sediments: Soil Sci. Soc. America Proc. v. 36, p. 279-285.

Li, Y. H., Bischoff, J. L., and Mathieu, G., 1969, The migration of manganese in the Arctic-Basin sediments: Earth Planetary Sci. Letters, v. 7, p. 265-270.

Li, Y. H., and Gregory, S., 1974, Diffusion of ions in sea water and in deep-sea sediments: Geochim. et Cosmochim. Acta, v. 38, p. 703-714.

Lyman, J., 1965, Apparent dissociation constants of carbonic acid, Appendix Tables VI-VIII, *in* Riley, J. P., and Skirrow, G., eds., Chemical Oceanography, v. 1: New York, Academic Press, 651 p.

Mangum, C. P., 1964, Activity patterns in metabolism and ecology of polychaetes: Comparative Biochemistry-Physiology, v. 11, p. 239-256.

Mann, P. J. G., and Quastel, J. H., 1946, Manganese metabolism in soils: Nature, v. 158, p. 154-156.

Mills, K. C., 1974, Thermodynamic data for inorganic sulfides, selenides, and tellurides: London, Butterworth & Sons, 845 p.

Morgan, J. J., 1967, Chemical equilibria and kinetic properties of manganese in natural waters, *in* Fuast, S. P., and Hunter, J. V., eds., Principles and Applications of Water Chemistry: New York, John Wiley & Sons, p. 561-622.

Mortimer, C. H., 1941, The exchange of dissolved substances between mud and water. I and II: Jour. Ecology, v. 29, p. 280-329.

Mortland, M. M., and Wolcott, A. R., 1965, Sorption of inorganic nitrogen compounds by soil materials, *in* Bartholomew, W. V., and Clark, F. E., eds., Soil Nitrogen: Agronomy, v. 10, p. 150-197.

Muskat, M., 1934, The flow of compressible fluids through porous media and some problems in heat conduction: Physics, v. 5, p. 71-94.

Myers, A. C., ms, 1973, Sediment reworking, tube building, and burrowing in a shallow subtidal marine bottom community: rates and effects: Ph.D. dissert., Univ. Rhode Island, Kingston, R. I., 117 p.

Nelson, H. M., 1952, Temperature distribution with simultaneous platten and dielectric heating: British Jour. Appl. Physics, v. 3, p. 79-86.

Nõmmik, H., 1965, Ammonium fixation and other reactions involving a nonenzymatic immobilization of mineral nitrogen in soil, *in* Bartholomew, W. V., and Clark, F. E., eds.: Soil Nitrogen: Agronomy, v. 10, p. 198-258.

Norvell, W. A., 1974, Insolubilization of inorganic phosphate by anoxic lake sediment: Soil Sci. Soc. America Proc., v. 38, p. 441-445.

Nriagu, J. O., 1972, Stability of vivianite and ion pair formation in the system $Fe_3(PO_4)_2$–H_3PO_4–H_2O: Geochim. et Cosmochim. Acta, v. 36, p. 459-470.

Nriagu, J. O., and Dell, C. I., 1974, Diagenetic formation of iron phosphates in recent lake sediments: Am. Mineralogist, v. 59, p. 934-946.

O'Malley, K. L., and Terwilliger, R. C., 1975, Aspects of nitrogen metabolism in the terebellid polychaete *Pista pacifica* Berkeley: Comparative Biochemistry Physiology, v. 52A, p. 367-369.

Oppenheimer, C. H., 1960, Bacterial activity in sediments of shallow marine bays: Geochim. et Cosmochim. Acta, v. 19, p. 244-260.

Parfitt, R. L., Atkinson, R. J., and Smart, R. St. C., 1975, The mechanism of phosphate fixation by iron oxides: Soil Sci. Soc. America Proc., v. 39, p. 837-841.

Presley, B. J., 1971, Techniques for analyzing interstitial water samples. Part I: Determination of selected minor and major inorganic constituents: Initial Repts. Deep Sea Drilling Project, v. 7, p. 2, p. 1749-1755.

Rhoads, D. C., 1963, Rates of sediment reworking by *Yoldia limatula* in Buzzards Bay, Massachusetts and Long Island Sound: Jour. Sed. Pet., v. 33, p. 723-727.

———— 1967, Biogenic reworking of intertidal and subtidal sediments in Barnstable Harbor and Buzzards Bay, Massachusetts: Jour. Geology, v. 75, p. 461-476.

Rhoads, D. C., Aller, R. C., and Goldhaber, M. B., 1977, The influence of colonizing macrobenthos on physical properties and chemical diagenesis of the estuarine seafloor, *in* Coull, B. C., ed., Ecology of marine benthos: Columbia, S.C. Press, Belle W. Baruch Library in Marine Science, no. 6, p. 113-138.

Rhoads, D. C., and Stanley, D. J., 1965, Biogenic graded bedding: Jour. Sed. Pet., v. 35, p. 956-963.

Rhoads, D. C., and Young, D. K., 1970, The influence of deposit-feeding organisms on sediment stability and community trophic structure: Jour. Marine Research, v. 28, p. 150-178.

Richards, F. A., 1965, Anoxic basins and fjords, *in* Riley, J. P., and Skirrow, G., eds., Chemical Oceanography, v. 1: New York, Academic Press, p. 611-645.

Rickard, D. T., 1969, The chemistry of iron sulfide formation at low temperatures: Stockholm, Contr. Geology, v. 20, p. 67-95.

Rosenfeld, J. K., ms, 1977, Nitrogen diagenesis in nearshore anoxic sediments: Ph.D. dissert., Yale Univ., New Haven, Conn., 191 p.

Sanders, H. L., 1956, Oceanography of Long Island Sound, 1952-1954. X. The biology of marine bottom communities: Bingham Oceanog. Colln. Bull., v. 15, p. 345-414.

Sholkovitz, E., 1973, Interstitial water chemistry of the Santa Barbara Basin sediments: Geochim. et Cosmochim. Acta, v. 37, p. 2043-2073.

Sillén, L. G., and Martell, A. E., 1964, Stability constants of metal-ion complexes: London, Burlington House, Chem. Soc. Spec. Pub. 17, 754 p.

Singer, P. C., and Stumm, W., 1970, Solubility of ferrous iron in carbonate bearing waters: Am. Water Works Assoc. Jour., v. 62, p. 198-202.

Solórzano, L., 1969, Determination of ammonia in natural waters by the phenol-hypochlorite method: Limnology Oceanography, v. 14, p. 799-801.

Sorokin, Yu. I., 1962, Experimental investigation of bacterial sulfate reduction in the Black Sea using S^{35}: Mikrobiologiya, v. 31, p. 402-410.

Stanley, S. M., 1970, Relation of shell form to life habits in the Bivalvia: Geol. Soc. America Mem. 125, 296 p.

Stookey, L. L., 1970, Ferrozine- a new spectrophotometric reagent for iron: Anal. Chem., v. 42, p. 779-781.

Strickland, J. D. H., and Parsons, T. R., 1969, A practical handbook of sea water analysis: Canada Fisheries Research Board, Bull., v. 167, 311 p.

Stumm, W., and Lee, G. F., 1961, Oxygenation of ferrous iron: Ind. Eng. Chem. 53, p. 143-146.

Stumm, W., and Morgan, J. J., 1970, Aquatic Chemistry: New York, John Wiley & Sons, 583 p.

Syers, J. K., Harris, R. F., and Armstrong, D. E., 1973, Phosphate chemistry in lake sediments: Jour. Environmental Quality, v. 2, p. 1-14.

Tessenow, U., 1974, Losungs-, Diffusions-, und Sorptionsprozesse in der Oberschicht von Seesedimenten. IV: Arch. Hydrobiol. Suppl. 47, p. 1-79.

Trimble, R. B., and Ehrlich, H. L., 1968, Bacteriology of manganese nodules. III. Reduction of MnO_2 by two strains of nodule bacteria: Appl. Microbiology, v. 16, p. 695-702.

Troup, B. N., ms, 1974, The interaction of iron with phosphate, carbonate and sulfide in Chesapeake Bay interstitial waters: A thermodynamic interpretation: Ph.D. dissert., The Johns Hopkins Univ., Baltimore, Md., 114 p.

Troup, B. N., Bricker, O. P., and Bray, J. T., 1974, Oxidation effect of the analysis of iron in the interstitial water of recent anoxic sediments: Nature, v. 249, p. 237-239.

Turekian, K. K., 1977, The fate of metals in the oceans: Geochim. et Cosmochim. Acta, v. 41, p. 1139-1144.

Vanderborght, J. P., Wollast, R., and Billen, G., 1977, Kinetic models of diagenesis in disturbed sediments. Part I. Mass transfer properties and silica diagenesis: Limnology Oceanography, v. 22, p. 787-793.

Waksman, S. A., and Hotchkiss, M., 1938, On the oxidation of organic matter in marine sediments by bacteria: Jour. Marine Research, v. 1, p. 101-118.

Yingst, J. Y., 1978, Patterns of micro- and meiofaunal abundance in marine sediments measured with the adenosine triphosphate assay: Marine Biology, v. 47, p. 41-54.

Young, D. K., 1971, Effects of infauna on the sediment and seston of a subtidal environment: Vie et Milieu, Suppl. 22, p. 557-571.

Zobell, C. E., and Anderson, D. Q., 1936, Vertical distribution of bacteria in marine sediments: Am. Assoc. Petroleum Geologist Bull., v. 20, p. 258-269.

Zobell, C. E., and Rittenberg, S. C., 1948, Sulfate reducing bacteria in marine sediments: Jour. Marine Research, v. 7, p. 602-617.